Helminth infections drive heterogeneity in human type 2 and regulatory cells*

Authors: Karin de Ruiter[1*], Simon P. Jochems[1*], Dicky L. Tahapary[1,2,3#], Koen A. Stam[1#], Marion König[1], Vincent van Unen[4], Sandra Laban[4], Thomas Höllt[5,6], Moustapha Mbow[7], Boudewijn P.F. Lelieveldt[8,9], Frits Koning[4], Erliyani Sartono[1], Johannes W.A. Smit[10,11], Taniawati Supali[12], Maria Yazdanbakhsh[1]†

*,[#]These authors contributed equally to this work.

† Corresponding author. Email: m.yazdanbakhsh@lumc.nl

Affiliations:

1 Department of Parasitology, Leiden University Medical Center, 2333 ZA Leiden, The Netherlands.

2 Department of Internal Medicine, Division of Endocrinology, Dr. Cipto Mangunkusumo National General Hospital, Faculty of Medicine Universitas Indonesia, 10430 Jakarta, Indonesia.

3 Metabolic, Cardiovascular and Aging Cluster, The Indonesian Medical Education and Research Institute, Universitas Indonesia, 10430 Jakarta, Indonesia.

4 Department of Immunohematology and Blood Transfusion, Leiden University Medical Center, 2333 ZA Leiden, The Netherlands.

5 Computer Graphics and Visualization Group, Delft University of Technology, 2628 XE Delft, The Netherlands.

6 Computational Biology Center, Leiden University Medical Center, 2333 ZA Leiden, The Netherlands.

7 Department of Immunology, Cheikh Anta Diop University of Dakar (UCAD), 5005 Dakar, Senegal.

8 Department of LKEB Radiology, Leiden University Medical Center, 2333 ZA Leiden, The Netherlands.

9 Department of Pattern Recognition and Bioinformatics Group, Delft University of Technology, 2628 XE Delft, The Netherlands.

10 Department of Internal Medicine, Radboud University Medical Centre, 6525 GA Nijmegen, The Netherlands.

11 Department of Internal Medicine, Leiden University Medical Center, 2333 ZA Leiden, The Netherlands.

12 Department of Parasitology, Faculty of Medicine Universitas Indonesia, 10430 Jakarta, Indonesia.

OVERLINE: PARASITIC INFECTIONS

One Sentence Summary: Mass cytometry identifies clusters of type 2 and regulatory immune responses in pre and post anthelmintic treatment human blood samples.

Editor's summary: Parasite perturbation of immunity
Helminths infect billions of people and are known to modulate host immune responses to promote their survival. De Ruiter et al. used mass cytometry to gain a better understanding of which cells are affected by helminth infection. They analyzed samples from Europeans or urban Indonesians, neither of which had been exposed to helminths. These were compared to samples from rural Indonesians before and after deworming treatment. Helminths expanded innate lymphoid type 2 cells, T helper type 2 cells, a subset of regulatory T cells, and IL-10 producing B cells. The immune alterations resolved upon deworming. These details on host-pathogen interaction could inform future targeted therapies.

Abstract

Helminth infections induce strong type 2 and regulatory responses, but the degree of heterogeneity of such cells is not well characterized. Using mass cytometry we profiled these cells in Europeans and Indonesians not exposed to helminths, and in Indonesians residing in rural areas, infected with soil-transmitted helminths. To assign immune alteration to helminth infection, the profiling was performed before and 1 year after deworming. Very distinct signatures were found in Europeans and Indonesians, showing expanded frequencies of Th2 cells, in particular $CD161^+$ cells, and ILC2s, in helminth-infected Indonesians, which was confirmed functionally through analysis of cytokine-producing cells. Besides ILC2s and $CD4^+$ T cells, $CD8^+$ T cells and γδ T cells in Indonesians produced type 2 cytokines. Regulatory T cells were also expanded in Indonesians, but only those expressing CTLA-4, and some co-expressed CD38, HLA-DR, ICOS, or CD161. $CD11c^+$ B cells were found to be the main IL-10 producers among B cells in Indonesians, a subset which was almost absent in Europeans. A number of the distinct immune profiles were driven by helminths as the profiles reverted following clearance of helminth infections. Moreover, Indonesians with no helminth infections residing in an urban area showed immune profiles that resembled Europeans rather than rural Indonesians, which excludes a major role for ethnicity.

Detailed insight into the human type 2 and regulatory networks could provide opportunities to target these cells for more precise interventions.

Introduction

There are considerable population differences in immune profiles (*1, 2*), which, although in part can be explained by genetic factors, seems to be largely driven by environmental exposures (*3, 4*). One such exposure is to helminths, which are ubiquitous in many parts of the world (*5*). Such parasites are known as the strongest natural inducers of type 2 immune responses (*6*) characterized by $CD4^+$ T helper 2 (Th2) cells secreting the hallmark cytokines interleukin (IL)-4, IL-5 and IL-13, as well as group 2 innate lymphoid cells (ILC2s), which are the predominant innate source of type 2 cytokines. Although ILC2s have been studied extensively in mice (*7-9*), it has been challenging to study these cells in humans due to their low frequency in peripheral blood (*10*). Together, these type 2 immune responses lead to eosinophilia, expansion of basophils and mast cells, goblet cell hyperplasia, and the production of IgE (*11*). There is evidence for a role of type 2 immune responses in controlling helminth parasites through killing or expulsion, and in inducing tissue repair, necessary to protect against damage caused by tissue-migrating helminths (*12*). However, there is increasing realization that type 2 cells might participate in maintaining physiological homeostasis, for example glucose metabolism or thermoregulation (*13*). It is also known that these cells can play a pathological role, for example in allergic diseases, such as asthma (*14*).

Besides polarizing the immune system towards a type 2 immune response, helminths can induce a strong regulatory network (*15-18*), which can enhance their survival within their host but at the same time affect responses to bystander antigens, such as allergens, autoantigens, or vaccines

(*19*). Regulatory T cells (Tregs), expressing FOXP3, are an important component of such a network, and mediate their effects through suppressive cytokines (e.g. IL-10 and TGF-β) and/or via the expression of suppressor molecules such as cytotoxic T lymphocyte antigen 4 (CTLA-4) (*20*). Although longitudinal studies assessing the effect of deworming on Tregs are rare, we recently found that not the Treg frequencies, but the expression of CTLA-4 on $CD4^+$ T cells significantly declined in anthelmintic-treated individuals (*21*).

Given the spectrum of immune modulatory effects that helminths exhibit, we believe that by understanding type 2 and regulatory responses in depth it will be possible to devise interventions that could help vaccine responses or curtail inflammation that damages tissues and organs in a more targeted manner.

With the advent of mass cytometry, it has become possible to capture the complex profile of immune cells (*22*). To better understand the helminth-modulated responses and identify cell populations that might be closely linked to this process, we performed immune profiling by mass cytometry with an emphasis on type 2 and regulatory responses, using simultaneous measurement of 37 cellular markers at the single-cell level to allow high-resolution dissection of the cellular composition. A well-established technique for mass cytometry data analysis is t-distributed Stochastic Neighbor Embedding (t-SNE) (*23*), which allows visualization of all concurrent marker expression profiles of cells on a two-dimensional plot in an unbiased fashion. However, t-SNE does not scale well to large amounts of data. Recently introduced techniques, such as Uniform Manifold Approximation and Projection (UMAP) (*24*) and Hierarchical Stochastic Neighbor Embedding (HSNE) (*25*) promise to overcome this scaling problem. Here, we applied HSNE, as implemented in Cytosplore (*26*), to visualize and cluster the data. These methods were applied to study type 2 and regulatory responses *ex vivo*, in addition to determining function in terms of

cytokine production in Europeans and helminth-infected Indonesians, before and one year after 3-monthly anthelmintic treatment, when they became free of helminth infection.

Results

Distinct immune signatures between Europeans and rural Indonesians

The first study cohort consisted of age- and sex-matched Europeans without prior exposure to helminths and Indonesians from a rural area, infected with soil-transmitted helminths before and after 1 year of deworming (table S1 and table S2). The 37-metal isotope-tagged monoclonal antibody panel (table S3) allowed the identification of six major immune lineages ($CD4^+$, $CD8^+$, γδ T cells, B cells, myeloid cells, and innate lymphoid cells (ILCs; $CD3^-CD7^+$)), and major subpopulations and detailed cell clusters within. Importantly, by using the t-SNE-based HSNE (*26*), we could explore the full mass cytometry dataset containing 20.3 million live $CD45^+$ cells at the single-cell level without the need for downsampling. At the overview level, landmarks (representative cells) depict the global composition of the entire immune system and distinguish the major immune lineages, which were annotated based on lineage marker expression overlays (Fig. 1A-B). Quantification of cell frequencies revealed a significantly higher frequency of B cells in Indonesians ($P < 0.05$), but no other differences were found between Europeans and Indonesians at the lineage level (Fig. 1C, fig. S1). Next, $CD4^+$ T cell landmarks, representing 6.3 million cells, were selected at the overview level and a new higher resolution embedding was generated at the second level of the hierarchy (Fig. 1D), revealing subpopulations within the $CD4^+$ T cell lineage (Fig. 1D). Stratification by origin of the samples revealed a strikingly different distribution of the $CD4^+$ T cells between Europeans and Indonesians, visualized by cell density plots (Fig. 1E). Different cellular distributions were also observed within other lineages ($CD8^+$, γδ T cells, B cells,

myeloid cells and ILCs) (Fig. 1E), suggesting very distinct immune signatures between Europeans and rural Indonesians in both the innate and adaptive immune compartment.

A CD161$^+$ subpopulation of Th2 cells is expanded in rural Indonesians and decreases after anthelmintic treatment

Within the CD4$^+$ T cells, a distinct population of Th2 cells was found that expressed GATA3, CD25, CD127, CD45RO and chemoattractant receptor-homologous molecule expressed on Th2 (CRTH2), the latter being the most reliable marker to identify human Th2 cells (*27*) (Fig. 2A). The frequency of total Th2 cells was higher in rural Indonesians compared to Europeans and importantly, deworming resulted in a decrease (Fig. 2B). This is in line with the observation that the proportion of circulating eosinophils as well as serum levels of total IgE, both markers of the type 2 response, significantly decreased in the helminth-infected Indonesians after treatment (Fig. S2, $P < 0.01$).

Further analysis of Th2 cells revealed 22 phenotypically distinct clusters using the Gaussian mean shift (GMS) clustering (Fig. 2C). Th2 cells showed considerable heterogeneity and based on the expression of the lectin-like receptor CD161 and CD27, the latter which is lost on highly differentiated memory CD4$^+$ T cells (*28, 29*), three subpopulations could be identified (CD161$^+$CD27$^-$, CD161$^-$CD27$^-$ and CD161$^-$CD27$^+$ Th2 cells; Fig. 2C-D). Visualization of Th2 cells by density plots (Fig. 2E) showed that the proportion of CD161$^+$ Th2 cells may have been expanded in rural Indonesians compared to Europeans, although the difference fell short of statistical significance, but a decrease was observed after anthelmintic treatment (Fig. 2F). Deeper analysis at the cluster level revealed three clusters within the CD161$^+$ Th2 population that declined upon deworming (Fig. 2G). These clusters were not only reciprocally expressing CD7 and KLRG1

(CD161^{+}CD7^{-}KLRG1^{+} and CD161^{+}CD7^{+}KLRG1^{-}), but also contained cells that did not express CD7 or KLRG1 (Fig. 2G), suggesting that helminth infection not only expanded effector cells in a more terminally differentiated state (*30*) but also CD161^{+} cells in transition . In contrast, after one year of treatment we observed an increase of three CD7^{+} Th2 clusters that only weakly expressed GATA3 and CRTH2 (Fig. 2G), suggesting an expansion of cells with lower type 2 cytokine production (*31, 32*).

The proportion of poorly differentiated CD27^{+} Th2 cells was higher in Europeans (Fig. 2F) and this difference was specifically in the CCR7^{-} cluster within the CD27^{+} Th2 cell subpopulation (Fig. 2G). This finding indicates that in contrast to rural Indonesians, the frequency of highly differentiated memory effector Th2 cells in the immune system of Europeans is low.

Overall frequency of ILC2s is expanded in rural Indonesians but does not decrease after anthelmintic treatment

The study of human helper-like ILCs has been difficult due to their low frequency in peripheral blood. However, using mass cytometry, it was possible to analyze these cells at a detailed level as part of 2.8 million ILCs (CD3^{-}CD7^{+}), which include NK cells as well (Fig. 3A). The embedding of a CD25^{+}CD127^{+}CD161^{+} subpopulation revealed 2 distinct clusters that were phenotyped as ILC2s and ILC3s, based on the expression of CRTH2 and c-Kit, respectively (Fig. 3A). It was found that other markers such as GATA3, KLRG1, CD45RA, and CCR6 could also be expressed by ILC2s and/or ILC3s (Fig. 3A). Consistent with previous work (*33*), we observed that whereas GATA3, the Th2 master transcription factor, was highly expressed in CRTH2^{+} ILC2s, it was also expressed in CRTH2^{-} ILCs and can therefore not exclusively be used to define ILC2s. In contrast to ILC3s, the proportion of ILC2s was higher in rural Indonesians compared to Europeans, but did

not decrease after anthelmintic treatment (Fig. 3B). Further characterization of ILC2s resulted in 8 phenotypically distinct clusters that could be distinguished by the expression of CD45RA, KLRG1, and CCR6 (Fig. 3C), showing more heterogeneity than what has been described so far based on the varying expression of KLRG1 and CCR6 on ILC2s (*34*). Moreover, the expression of CCR6, involved in gut homing (*35*), has been seen on peripheral blood ILC2s in patients with inflamed tissues (*36*). Interestingly we observe a lower frequency of $KLRG1^{+}CCR6^{+}$ ILC2s (cluster 5) in Indonesians infected with helminths residing in the GI tract, compared to Europeans (Fig. 3D).

Helminth infections increase the expression of inhibitory molecules on Tregs

Tregs characterized as $FOXP3^{+}CD25^{high}CD127^{low}$ cells appeared as a clearly distinct subpopulation within $CD4^{+}$ T cells (Fig. 4A). The frequency of Tregs, when assessed as a whole, did not differ between Europeans and Indonesians, nor changed after deworming (Fig. 4B). However, the immune profile of rural Indonesians consisted of more effector Tregs expressing CD45RO (Fig. 4C), whereas in Europeans, a clear population of Tregs was positioned in the naïve, $CD45RA^{+}$, compartment (Fig. 4D). In line with previous studies describing Tregs as phenotypically and functionally heterogeneous (*20*), we found several subpopulations within the effector Treg compartment expressing CTLA-4, HLA-DR, CD38, and/or ICOS (Fig. 4E). A substantial proportion of the effector Tregs expressed CTLA-4, a marker that is associated with the suppressive function of Tregs (*37*). In concordance with this, the proportion of $CTLA\text{-}4^{+}$ Tregs was higher in rural Indonesians compared to Europeans and decreased after anthelmintic treatment (Fig. 4F).

Next, we identified 27 phenotypically distinct clusters within Tregs (Fig. 4G-H). Analysis at the cluster level revealed that the frequencies of 6 out of 27 clusters were higher in rural Indonesians compared to Europeans, distinguished by the expression of only CTLA-4, or co-expression of CD38 and/or HLA-DR and/or ICOS (Fig. 4H). One of these clusters (cluster 7) expressing CTLA-4, HLA-DR, CD38, and ICOS, decreased upon deworming, suggesting that this population of effector Tregs is particularly important in the immune response induced by helminths . Of note, among the CTLA-4$^+$ Tregs, we identified a cluster expressing CD161 (cluster 25; Fig. 4H). CD161$^+$ Tregs were recently described as a highly suppressive, cytokine-producing population of Tregs that was enriched in the intestinal mucosa, particularly in inflammatory bowel disease, where they can enhance wound repair (*38*). The proportion of CD161$^+$ Tregs was higher in rural Indonesians compared to Europeans but did not change after deworming (Fig. 4I), suggesting that factors other than helminth infections might be associated with the presence of such cells.

Type 2 cytokine-producing cells in rural Indonesians (ILC2s, CD4$^+$, CD8$^+$ and γδ T cells) and their alteration after deworming

Following the phenotypic characterization of type 2 cells, the cytokine production of PMA/ionomycin-stimulated cells was analyzed through a second CyTOF panel (Table S4) which included IFNγ, TNFα, IL-2, IL-17, IL-10 and IL-4/IL-5/IL-13 (simultaneously assessed and hereafter referred to as 'type 2 cytokines'), to assess their functional capacity. Type 2 cytokine-producing CD45$^+$ cells were analyzed in Cytosplore and clustering on surface markers revealed striking differences between Europeans and helminth-infected Indonesians (Fig. 5A-C). Overall four distinct type 2 cytokine-producing subpopulations were identified (Fig. 5D, Fig. S3) of which

$CD4^+$ T cells and ILC2s showed the greatest per-cell type 2 cytokine expression (Fig. 5E).Whereas the $CD25^-$ proportion of $CD4^+$ and $CD8^+$ T cells and all γδ T cells co-expressed IFNγ with the type 2 cytokines, ILC2s did not (Fig. 5E-F). Helminth-infected rural Indonesians exhibited a higher frequency of total type 2 cytokine-producing cells compared to Europeans and this trend was consistently observed for the individual subpopulations (Fig. 5G-H), suggesting that helminths expand the cellular sources for these cytokines. Importantly, the proportion of type 2 cytokine-producing cells declined after deworming (Fig. 5G) and this was attributed to a decrease in type 2 cytokine-producing $CD4^+$ T, $CD8^+$ T cells and ILC2s (Fig. 5H).

The proportion of type 2 cytokine-producing $CD8^+$ T cells correlated strongly with a subset previously defined as type 2 cytotoxic T (Tc2) cells (*39, 40*) (r=0.87, $P < .001$), which were phenotypically identified as a $GATA3^+$ cluster within a subpopulation of $CD45RO^+CCR7^-CD161^-$ $CD56^-$ $CD8^+$ T cells (2.1% of $CD8^+$ T cells), expressing CRTH2, CD25, CD127 and CD7 (Fig. 6). However, it should be noted that the frequency of Tc2 cells varied considerably, from 0.09 to 16.8% of $CD8^+$ T cells, in different individuals. Although there was a decrease in type 2 cytokine-producing $CD8^+$ cells, there was no decrease in Tc2 cells after deworming, which might indicate that factors other than helminths can induce these cells, or historical rather than current exposure to helminths is more decisive in driving the expansion of these cells.

IL10-producing B and $CD4^+$ T cells revealed by mass cytometry

Similarly, we sought cells that produced the suppressor cytokine IL-10 to further understand the regulatory network. The IL-10-producing $CD45^+$ cells were analysed in Cytosplore (Fig. 7A-B) and clustering on surface markers revealed a major cluster of $CD4^+$ T cells, and minor clusters of $CD8^+$ T cells, $CD4^-CD8^-$ T cells and B cells (Fig. 7C-D, Fig. S4). Unlike what was seen with

CTLA-4 expression, no differences in frequencies of total IL-10-producing cells (relative to $CD45^+$ cells) were observed among Europeans and rural Indonesians (EU 0.5% (median), ID Pre 0.5% of total $CD45^+$ cells, $P = 0.86$), and these did not change after anthelmintic treatment (ID Pre 0.4 % of total $CD45^+$ cells, $P = 0.40$).

Interestingly, a distinct population of IL-10^+ B cells (0.5% of total B cells) was identified and further analysis showed that it consisted of three clusters, namely $CD11c^+CD38^-$, $CD11c^-CD38^+$ and $CD11c^-CD38^-$ cells (Fig. 7E). Whereas the composition of IL-10^+ B cells did not change after deworming, IL-10^+ B cells from rural Indonesians clearly contained more $CD11c^+CD38^-$ cells compared to Europeans, who had relatively more $CD11c^-CD38^+$ IL-10^+ B cells (Fig. 7F). These results indicate a different phenotype of IL-10^+ B cells in the two populations, which is in line with significantly more $CD11c^+$ B cells, representing chronically stimulated cells, in rural Indonesians compared to Europeans (EU 5.0% (median), ID Pre 13% of total B cells, $P < 0.01$).

When IL-10-producing $CD4^+$ T cells were clustered on cytokines, four clusters were identified which all expressed type 2 cytokines but varied in terms of co-expression of other cytokines (IFNγ, TNFα, and/or IL-2) (Fig. 7G-H). When considering all $CD4^+$ T cells producing IL-10 and type 2 cytokines, irrespective of other cytokines, their frequency was higher in rural Indonesians compared to Europeans. However, only the IL-10 and type 2 cytokine-producing cluster that was negative for IFNγ, TNFα, and IL-2 (cluster 1) decreased after deworming (Fig. 7I).

The immune profile of urban Indonesians resembles that of Europeans rather than rural Indonesians

We next sought to assess whether ethnic differences were driving the observed differences between Europeans and rural Indonesians. Therefore, we analysed a second cohort of eight Europeans eight Indonesians from urban centers, such as central Jakarta, where helminth infections are not found (urban Indonesians) (*41*), and eight Indonesians from the rural setting with current helminth infection (rural Indonesians) (table S1 and table S2). The same CyTOF panels and analysis strategy were used for the 14.3 million unstimulated and 12.2 million stimulated cells measured in this independent cohort (Fig. 8 and Fig. S5 and S6).

Increased frequencies of Th2 cells were present in Rural Indonesians compared to both European and urban Indonesians (Fig. 8A). Within Th2 cells, rural Indonesians had increased levels of $CD161^+$ cells compared to Europeans and urban Indonesians (Fig. 8C,D). Although in this independent cohort total ILC2 frequencies were not increased in rural Indonesians based on surface markers (Fig. S5D), ILC2 subsets differed between populations (Fig. 8D). Similar to the initial cohort, rural Indonesians, and also urban Indonesians, had increased $CCR6^-KLRG1^+$ ILC2s compared to Europeans. Functionally, ILC2 and Th2 cells were also increased in rural Indonesians as increased type 2 cytokines were produced compared to Europeans, whereas urban Indonesians resembled Europeans (Fig. 8E,F).

As observed in the original cohort, rural Indonesians had increased proportions of $CD161^+$ and CTLA-4^+ Tregs compared to Europeans and urban Indonesians (Fig. 8G,H). Total Tregs were also increased in rural Indonesians in this cohort compared to Europeans (Fig. S5E). IL-10^+ B cells of rural Indonesians in the independent cohort were characterized by increased expression of CD11c compared to Europeans and urban Indonesians as in the original cohort (Fig. 8H,I).

Taken together, we found urban Indonesians resembled Europeans more closely than rural Indonesians, demonstrating that ethnic differences were not driving the altered immune profiles . Moreover, we were able to validate the main findings of altered type 2 and regulatory immune cell populations in an independent cohort.

A summary of the heterogeneity of the type 2 and regulatory cell phenotypes, and the type 2-cytokine and IL-10 producing cells that align with Europeans, rural helminth-infected Indonesians (before and after anthelmintic treatment) and urban Indonesians is given in fig. S6.

Discussion

Our study used mass cytometry to analyze type 2 and regulatory immune cells of healthy Europeans, as well as of helminth-infected Indonesians before and one year after deworming, to start to understanding the heterogeneity in the immune response of populations living in different geographical areas. We have identified and shown the expansion of not only Th2 but also the rare ILC2 cells, both sources of type 2 cytokines, in helminth-infected Indonesians compared to Europeans. When considering the cells by their phenotype, Th2 cell frequencies significantly decreased after deworming, but the frequencies of ILC2s remained unchanged. However, the frequency of not only Th2 but also ILC2s producing type 2 cytokines declined after anthelmintic treatment, indicating decreased functional activity. There is very little known about the role of ILC2s in human helminth infections (*43*, *44*). Although the identification of CRTH2 as a marker of human ILC2s has been a great advantage (*45*), only one study analyzed ILC2s using CRTH2 in the context of human helminth infection *(44)*. This study found lower frequencies of ILC2s in *Schistosoma haematobium*-infected African children but in line with the trend in our study, the proportion of ILC2s increased 6 weeks after anthelmintic treatment (*44*).

We identified 8 ILC2 clusters based on the heterogeneous expression of KLRG1, CD45RA and CCR6, paving the way for future studies to investigate their specific function. Interestingly, we identified $CD45RA^{+}$c-Kit^{+} ILC3s that did not express CCR6, a marker previously described to be expressed by ILC3s (*33, 46*), and hypothesize that this subpopulation might consist of the recently described ILC precursors, as these cells lack CCR6 expression and are $CD45RA^{+}$ (*47*).

There is increasing evidence for the heterogeneity of Th2 cells, for example, pathogenic effector Th2 (peTh2) cells have recently been found in patients with allergic eosinophilic inflammatory diseases, that have enhanced effector function as assessed by cytokine production (*48, 49*). It is thought that chronic antigen exposure drives peTh2 cells, characterized as $CD161^{+}hPGDS^{+}CD27^{-}$, to differentiate from conventional Th2 cells, however, it is not known whether peTh2 cells are induced by human helminth infections (*49*). Here, we describe the increase of a peTh2-like $CD27^{-}CD161^{+}$ subset of Th2 cells in helminth-infected individuals which significantly decreased after deworming. Given the general lack of severe allergic diseases in rural areas where helminths are endemic (*50*), it would be interesting to assess whether in subjects chronically infected with helminths these cells, have a more regulated function and thus less pathogenic activity.

Tregs have been described as a heterogeneous population with differing expression of HLA-DR (*51*), ICOS (*52*) and CD38 (*53*) within the $FOXP3^{+}$ Treg population. Functionally, Tregs expressing HLA-DR or CD38 have been shown to be highly suppressive (*51, 53*) and whereas the expression of ICOS has been suggested to define a Treg subset that has the capacity to produce large amounts of IL-10, $ICOS^{-}$ Tregs seem to produce mainly TGF-β (*52*). Moreover, a recent study has reported an interesting subset of Tregs expressing CD161 (*38*). By using mass cytometry, we could not only confirm the presence of these distinct Treg phenotypes in our study population,

but also visualize the marker distribution which revealed that all HLA-DR$^+$, ICOS$^+$, CD38$^+$ and CD161$^+$ cells were found within the CTLA-4$^+$ Treg subset.

Although total Treg frequencies were not expanded in helminth-infected individuals and no treatment-related change was observed, when considering them at the subset level, the proportion of CTLA-4$^+$ Tregs was significantly higher in helminth-infected individuals and declined after treatment, consistent with previous work in children from the same study area (*18, 21*). Analysis at the cluster level revealed that the CTLA-4$^+$ clusters in particular, often co-expressing ICOS and/or HLA-DR and/or CD38, were expanded in rural Indonesians compared to Europeans, indicating that helminths induce a particular Treg phenotype which could be represented by cells with increased regulatory capacity (*21*). We also found a significantly higher proportion of CD161$^+$ Tregs in rural Indonesians compared to Europeans and given that this population was shown to accelerate epithelial barrier healing in the gut (*38*), they might play a role in healing of the wounds caused by soil-transmitted helminths, either during their migration throughout the body or upon their residence in the intestine.

Besides Th2 cells and ILC2s being a source of type 2 cytokines, we identified Tc2 cells (type 2 cytokine-secreting CD8$^+$ T cells (*39*)) and a cluster of γδ T cells, which produced type 2 cytokines. Although Tc2 cells have recently been found to be enriched in patients with eosinophilic asthma (*40*), this current study characterizes these cells in the context of human helminth infections. Like Tc2 cells, not much is known about type 2 cytokine-producing γδ T cells, although their existence has been described before (*54-58*). Inagaki et al. showed a protective role of γδ T cells against infection with *N. brasiliensis* in mice, which was associated with the production of type 2 cytokines, in particular IL-13 (*55*). However, to our knowledge, the presence of type 2 cytokine-producing γδ T cells in human helminth infection has not been previously reported. With

the increasing recognition of the role γδ T cells play in shaping adaptive responses in infectious diseases (*59, 60*), it would be interesting to delineate their possible participation in the development of Th2 responses.

IL-10 producing B cells, known as regulatory B cells (Bregs), represent a relatively rare cell type that can suppress inflammatory responses (*61*). The frequency of IL-10 producing B cells was similar in Europeans and Indonesians and deworming did not affect their frequency. However, the phenotype of these cells was strikingly different with relatively more $CD11c^{+}CD38^{-}$, and less $CD11c^{-}CD38^{+}$ $IL\text{-}10^{+}$ B cells present in Indonesians. There is increasing evidence that $CD11c^{+}$ B cells are a distinct population of memory B cells, and they have been shown to expand in settings of chronic infections such as HIV, malaria and TB as well as in several autoimmune diseases (*62, 63*). Our finding of a significantly expanded population of $CD11c^{+}Tbet^{+}$ B cells in Indonesians with chronic helminth infection, of which a small fraction appeared capable of producing IL-10, indicates that through the use of mass cytometry, it becomes possible to identify novel cell types that would need to be investigated for their properties including suppressor functions.

Here, we demonstrate the advantage of using mass cytometry combined with HSNE, which allowed the identification of rare cell populations, such as ILC2s, Tc2 cells and Bregs, and provided an opportunity to analyze the heterogeneity within Th2 cells and Tregs. A comparison of urban and rural Indonesians and Europeans demonstrates that the alterations in type 2 and regulatory immune cells were not due to ethnic differences as immune profiles of Indonesians resembled that of Europeans more than rural Indonesians. A strength of this study is that we validated these findings in an independent cohort, demonstrating the robustness of these findings. Limitations of our study include analyzing peripheral immune cells from a relatively small number of individuals. Additionally, there is a lack of placebo-treated individuals and the possibility that

other infections are affected by deworming. However, this study is a stepping stone to verify the findings in larger studies that allow detailed delineation of their function not only in helminth infections but also in other disease settings.

Materials and Methods

Study design

The objective of this study was to profile type 2 and regulatory immune responses in Europeans and in helminth-infected Indonesians, before and 1 year after deworming, by applying mass cytometry on peripheral blood samples. The Indonesian samples were part of the SugarSPIN trial, a household-based cluster-randomized double-blind trial that was conducted in three rural villages in Nangapanda, Ende district of Flores island (East Nusa Tenggara), Indonesia (*64*). The trial was approved by the ethics committee of Faculty of Medicine, Universitas Indonesia (FKUI) (ref: 549/H2·F1/ETIK/2013), and filed by the ethics committee of Leiden University Medical Center (LUMC). The trial is registered as a clinical trial (Ref: ISRCTN75636394). Written informed consent was obtained from participants prior to the study.

We were interested in subjects who were helminth-infected and successfully treated with albendazole (n=56). The treatment consisted of a single tablet of albendazole (400 mg; PT Indopharma Pharmaceutical, Bandung, Indonesia) for three consecutive days, and this regimen was given every three months for a total of four rounds (maximum of 12 tablets in total), between

May 2014 and February 2015. Before the start of drug administration and 6 weeks after the last round of drug administration, blood and stool samples were collected as previously described (*64*). To ensure that the subjects that were studied were unlikely to have become re-infected (subpatently), we selected subjects in whom eosinophils and IgE were decreased after treatment (n=10). Finally, age- and sex-matched samples of healthy volunteers, from the Netherlands (Caucasians) or from urban centers in Indonesia, such as central Jakarta, with no helminth infections were included in the study (Table S1 and Table S2). Primary data are reported in data file S1.

Parasitology

Aliquots of fresh stool samples were frozen at -20°C in the field study centre and subsequently at -80°C at the Department of Parasitology of FKUI and LUMC for DNA extraction. Stool DNA isolation and real-time PCR were performed pairwise (baseline and follow-up). DNA isolation from stool was performed as described elsewhere (*65*). Multiplex real-time polymerase chain reaction (PCR) was performed to simultaneously detect the presence of hookworm (*Ancylostoma duodenale*, *Necator americanus*), *Ascaris lumbricoides*, *Trichuris trichiura*, and *Strongyloides stercoralis*, using a method described previously (*65*). Stool samples were considered positive by PCR when cycle threshold (Ct) values were <50.

Eosinophil count and total IgE

A Giemsa-stained peripheral thin blood smear was read to assess the differential white blood cell count, resulting in a relative percentage of basophils, eosinophils, neutrophils, lymphocytes and monocytes. Total IgE was measured in serum as described previously (*66*).

PBMC cryopreservation

After diluting heparinised venous blood 2x with HBSS, PBMCs were isolated using Ficoll density gradient centrifugation within 12 hours after blood collection. The HBSS contained 100 U/mL penicillin G sodium and 100 µg/mL streptomycin. After washing twice with HBSS, the PBMCs were cryopreserved in RPMI 1640 containing 20% of heat-inactivated fetal calf serum (FCS; Bodinco) and 10% dimethyl sulfoxyde (DMSO). The RPMI medium contained 1 mM pyruvate, 2 mM L-glutamine, penicillin G and streptomycin. Cryovials containing the cell suspension were transferred to a Nalgene Mr Frosty Freezing Container (Thermo Scientific) which was placed at a -80°C freezer for a minimum of 4 hours. Subsequently, vials were stored in liquid nitrogen until analysis. The cryopreserved PBMCs collected in the field were shipped in a liquid nitrogen dry vapor shipper from Jakarta, Indonesia, to Leiden, the Netherlands, for analysis.

Mass cytometry antibody staining

Two antibody panels were designed to 1) phenotype immune cells *ex vivo* and 2) assess cytokine production after 6 hours of stimulation with phorbol 12-myristate 13-acetate (PMA) and ionomycin. Details on antibodies used are listed in tables S3 and S4. Antibody-metal conjugates were either purchased or conjugated using a total of 100 µg of purified antibody combined with the MaxPar X8 Antibody Labelling Kit (Fluidigm) according to manufacturer's protocol V7. The conjugated antibody was stored in 200 µL Antibody Stabilizer PBS (Candor Bioscience, GmbH) at 4°C. All antibodies were titrated on study samples.

On the day of the staining, cryopreserved PBMCs were thawed with 50% FCS/RPMI medium at 37°C and washed twice with 10% FCS/RPMI medium. Next, $3x10^6$ cells per sample,

used for phenotyping (Panel 1), were stored on ice temporarily while another $3x10^6$ cells per sample were transferred to 5 ml round-bottom Falcon tubes (BD Biosciences) for 6 hours of incubation in 10% FCS/RPMI with 100 ng/mL PMA (Sigma) and 1 µg/mL ionomycin (Sigma). After 2 hours of incubation at 37°C, 10 µg/mL brefeldin A (Sigma) was added after which the cells were incubated for 4 more hours. Subsequently, the cells were washed with PBS and resuspended in MaxPar staining buffer (Fluidigm) before continuing with the antibody staining (Panel 2).

For phenotyping (Panel 1), the staining was based on MaxPar Nuclear Antigen Staining Protocol V2 (Fluidigm). First, cells were washed with MaxPar staining buffer and centrifuged for 5 minutes at 300g in 5 mL eppendorf tubes. Then, the cells were incubated with 1 mL 500x diluted 500 µM Cell-ID Intercalator-103Rh (Fluidigm) in staining buffer at room temperature for 15 minutes to identify dead cells. After washing with staining buffer, cells were incubated with 5 µL Human TruStain FcX Fc-receptor blocking solution (BioLegend) and 40 µL staining buffer at room temperature for 10 minutes. Then, 50 µL of freshly prepared surface antibody cocktail was added and incubated at room temperature for another 45 minutes. Subsequently, cells were washed 2x with staining buffer and fixed and permeabilized using the eBioscience FOXP3/Transcription factor staining buffer set (eBioscience). After cells were incubated with 1 mL of the freshly prepared Fix/Perm working solution (prepared according to the manufacturer's instructions) for 45 minutes, cells were washed 2x with 1x Permeabilization buffer at 800g for 5 minutes. Next, 50 µL of the intranuclear antibody cocktail was added to 50 µL of cells resuspended in 1x Permeabilization buffer and incubated for 30 minutes at room temperature. Following the incubation, cells were washed once with 1x Permeabilization buffer and twice with staining buffer, before being stained with 1 mL 1000x diluted 125 µM Cell-ID Intercalator-Ir (Fluidigm) in

MaxPar Fix and Perm buffer (Fluidigm) at 4°C overnight to stain all cells. After 3 washes with staining buffer and centrifugation at 800 g, cells were stored as a pellet at 4°C and measured within 2 days.

To assess the cytokine production of PBMCs (Panel 2), the staining was based on MaxPar Cytoplasmic/Secreted Antigen Staining Protocol V3. While the surface staining was performed exactly as described above, cells were afterwards fixed by incubating them with 1 mL of freshly prepared 1x MaxPar Fix I buffer (Fluidigm) for 20 minutes at room temperature. Next, cells were washed 3x with MaxPar Perm-S buffer (Fluidigm) and 50 µL of cytokine antibody cocktail was added to 50 µL of cell suspension and incubated for 40 minutes at room temperature. Then, cells were washed 3x with staining buffer and stained with Cell-ID Intercalator-Ir as described above.

Mass cytometry data acquisition

Measurement of samples was randomised per subject to avoid bias, but samples belonging to the same subject were stained and measured together. Samples were measured with a Helios mass cytometer (Fluidigm), which was automatically tuned according to Fluidigm's recommendations. Before measuring, cells were counted, washed with Milli-Q water, passed over a cell strainer, and brought to a concentration of $1.0x10^6$ cells/mL with 10% EQ Four Element Calibration Beads (Fluidigm) in Milli-Q water. Mass cytometry data were acquired and analysed on-the-fly, using dual-count mode and noise-reduction on. Next to channels to detect antibodies, channels for intercalators (103Rh, 191Ir, 193Ir), calibration beads (140Ce, 151Eu, 153Eu, 165Ho, and 175Lu) and background/contamination (133Cs, 138Ba, 206Pb) were acquired. After data acquisition, the mass bead signal was used to normalize the short-term signal fluctuations with the reference EQ

passport P13H2302 during the course of each experiment. When applicable, normalized FCS files were concatenated using Helios software, without removing beads.

Mass cytometry data analysis

FlowJo V10 for Mac (FlowJo LLC) was used to gate out beads and we discriminated live, single $CD45^+$ immune cells with DNA stain and event length. The selected cells were exported as FCS files and analysed using HSNE (*25*), as implemented in Cytosplore (*26, 67*). HSNE constructs a hierarchy of non-linear similarities that can be interactively explored with a stepwise increase in detail up to the single-cell level (*26*). Briefly, the data exploration starts with the visualization of the embedding at the highest level, the overview level, where the layout of the landmarks (representative cells) indicates similarity in the high-dimensional space. The landmark size reflects its area of influence (AoI), containing cells that are well-represented by the landmark, and the similarity of two landmarks is defined as the overlap of their respective AoIs. Colouring of the landmarks is used to represent marker expressions. At the overview level, a group of landmarks (also referred to as cluster) can be selected, by manual gating based on visual cues such as marker expression, or by performing unsupervised Gaussian mean shift (GMS) clustering (*67, 68*) of the landmarks based on the density representation of the embedding. Next, we can zoom into this selection by means of a more detailed embedding and visualize all selected landmarks in a next level. While this process can be repeated until the data level is reached where each dot represents a single cell, this is not imperative and we often clustered at an intermediate level without reaching the data level. The number of hierarchical levels depended on the input-data size.

Before HSNE was applied, data were transformed using a hyperbolic arcsin with a cofactor of 5. Furthermore, within Cytosplore, an extra channel called 'SampleTag' was added to the FCS files to be able to identify from which sample an event originated after HSNE.

Clusters produced in Cytosplore were analysed using R software (R x64 version 3.5.1; R Foundation for Statistical Computing) and RStudio (Rstudio, Inc). The package 'cytofast' was used to produce heatmaps, scatterplots showing subset abundance and histograms showing the median signal intensity distribution of markers (*69*).

Statistical Analysis

Statistical analyses were performed using R software. To compare subpopulation and cluster abundance between Europeans and Indonesians pre-treatment unpaired *t* tests were used. Paired t tests were applied to compare pre- and post-treatment samples of Indonesians. Total IgE and eosinophil counts were log-transformed for analysis and paired *t* tests were used in GraphPad Prism (GraphPad Software). Spearman's correlation was used to assess the relationship between the frequency of Tc2 cells and type 2 cytokine-producing $CD8^+$ T cells. P values < 0.05 were considered statistically significant. For comparison of three groups in the second cohort, ANOVA followed by Tukey's post-test were used with one-sided testing based on the differences identified in the first cohort.

Supplementary Materials

Fig. S1. Lineage frequencies.

Fig. S2. Eosinophil counts and total IgE in rural Indonesians.

Fig. S3. Type 2-cytokine producing cells.

Figure legends

Figure 1. Distinct immune signatures between Europeans and Rural Indonesians. (**A**) First HSNE level embedding of 20.3 million peripheral immune cells from Europeans (n=10) and rural Indonesians infected with helminths (n=10), before and after 1 year of deworming. In all figures, color represents arsin5-transformed marker expression as indicated. Size of the landmarks represents area of influence (AoI). (**B**) The major immune lineages, annotated on the basis of lineage marker expression. (**C**) Comparison of lineage proportions relative to total cells between Europeans (EU) and rural Indonesians (ID). Differences between EU and ID were tested with Student's *t* test. **P* <0.05. (**D**) Second HSNE level embedding of the $CD4^+$ landmarks selected from the overview level of total PBMCs, as indicated by the red circle. Both landmarks (left panel) and the density features of the $CD4^+$ T cells (right panel) are shown. Density is indicated by color. (**E**) Density plots per lineage, stratified by sample origin.

Figure 2. A $CD161^+$ subpopulation of Th2 cells is expanded in rural Indonesians and decreases after anthelmintic treatment. (**A**) Fourth HSNE level embedding of the $CRTH2^+$ landmarks (Th2 cells) selected from the second HSNE level embedding of 6.3 million $CD4^+$ T cells, as indicated by the black circle. All cells in third level were selected for the fourth level. (**B**) Frequency of Th2 cells relative to $CD4^+$ T cells. Differences between EU (n=10) and rural ID pre-treatment (ID Pre, n=10) were tested with Student's *t* test, whereas differences between ID Pre and ID Post (n=10) were assessed using paired *t* tests. ***P* <0.01. (**C**) Cluster partitions of Th2 cells using density-based GMS clustering. The black circle indicates three subpopulations. (**D**) Marker expression of CD27 and CD161 on Th2 cells. (**E**) Density features of Th2 cells. (**F**) Frequency of three Th2 subpopulations ($CD161^+CD27^-$, $CD161^-CD27^-$, $CD161^-CD27^+$) relative to total Th2 cells. **P* <0.05. (**G**) A heatmap summary of median expression values (same colour coding as for the embeddings) of cell markers expressed by $CRTH2^+$ clusters identified in Fig. 2C and hierarchical clustering thereof. To compare cluster abundance between EU and ID Pre Student's *t* test was used, whereas paired *t* test was used to compare ID Pre and ID Post. Coloured symbols below the clusters indicate statistical significance.

Figure 3. Overall frequency of ILC2s is expanded in rural Indonesians but does not decrease after anthelmintic treatment. (**A**) The right panel shows the third HSNE level embedding of the

$CD25^+CD161^+CD127^+$ landmarks selected from the second HSNE embedding of 2.8 million ILCs ($CD3^-CD7^+$) shown in the left panel, and indicated by the black circle. (**B**) Frequency of ILC2s relative to total $CD45^+$ cells. Differences between EU (n=10) and ID Pre (n=10) were tested with Student's *t* test, whereas differences between ID Pre and ID Post (n=10) were assessed using paired *t* tests. ***P* <0.01. (**C**) Data level embedding of ILC2s. The upper left panel shows the cluster partitions using GMS clustering, whereas the other panels show the expression of KRLG1, CCR6 and CD45RA. (**D**) A heatmap summary of median expression values (same colour coding as for the embeddings) of cell markers expressed by ILC2 cell clusters identified in Fig. 3C. and hierarchical clustering thereof. To compare cluster abundance between EU and ID Pre Student's *t* test was used, whereas paired *t* test was used to compare ID Pre and ID Post. Coloured symbols below the clusters indicate statistical significance.

Figure 4. Helminth infections increase the expression of inhibitory molecules on Tregs. (**A**) Fourth HSNE level embedding of the $FOXP3^+$ landmarks (Tregs) selected from the second HSNE embedding of 6.3 million $CD4^+$ T cells, as indicated by the black circle. All cells from the third level were selected. (**B**) Frequency of Tregs relative to $CD4^+$ T cells. Differences between EU (n=10) and ID Pre (n=10) were tested with Student's *t* test, whereas differences between ID Pre and ID Post (n=10) were assessed using paired *t* tests. (**C**). Frequency of $CD45RO^+$ effector Tregs relative to total Tregs. **P* <0.05. (**D**) Density features of Tregs. (**E**) Marker expression of CTLA-4, ICOS, CD38, HLA-DR and CD161 by Tregs. (**F**) Frequency of CTLA-4^+ Tregs relative to total Tregs. **P* <0.05; ***P* <0.01. (**G**) Treg cluster partitions using GMS clustering. (**H**) A heatmap summary of median expression values (same colour coding as for the embeddings) of cell markers expressed by $FOXP3^+$ Treg clusters identified in Fig. 4G. and hierarchical clustering thereof. To compare cluster abundance between EU and ID Pre Student's *t* test was used, whereas paired *t* test was used to compare ID Pre and ID Post. Coloured symbols below the clusters indicate statistical significance. (**I**) Frequency of $CD161^+$ Tregs relative to total Tregs. **P* <0.05.

Figure 5. Type 2 cytokine-producing cells (ILC2s, $CD4^+$, $CD8^+$ and γδ T cells) and their alteration after deworming in rural Indonesians. (**A**) IL-4/5/13^+ cells were manually gated using Flowjo. Data from one representative individual is shown. (**B**) First HSNE level embedding of total IL-4/5/13^+ cells, clustered on surface markers. (**C**) Density features of IL-4/5/13^+ cells. (**D**)

The major immune cell subpopulations producing type 2 cytokines, annotated on the basis of lineage marker expression (*See Fig. S3*). (**E**) Histogram showing the median signal intensity (MSI) distribution of IL-4/5/13 and IFNγ for the subpopulations identified in Fig. 5D. (**F**) Marker expression of CD25 and IFNγ by IL-4/5/13$^+$ cells. (**G**) Frequency of total IL-4/5/13-producing cells relative to total CD45$^+$ cells. Differences between EU (n=10) and ID Pre (n=10) were tested with Student's *t* test, whereas differences between ID Pre and ID Post (n=10) were assessed using paired *t* tests. ***P* <0.01. (**H**) Frequency of IL-4/5/13-producing clusters identified in Fig. 5D. relative to total CD4$^+$ T, ILC2, γδ T or CD8$^+$ T cells. **P* <0.05; ***P* <0.01.

Figure 6. Tc2 cells are the source of type 2 cytokines produced by CD8$^+$ T cells. (**A**) CCR7$^-$ CD161$^-$CD56$^-$ landmarks were selected from the second level HSNE embedding of CD8$^+$ T cells, as indicated by the black circle. (**B**) From the next level embedding, GATA3$^+$ landmarks were selected and their marker expression is shown at the fourth level embedding.(C) Correlation of type 2 cytotoxic T (Tc2) cells identified in B-C and IL-4/5/13-producing CD8$^+$ T cells identified in Fig. 5D. Colors indicate paired samples (pre and post treatment) from Indonesian individuals (n=10), black dots represent European individuals (n=10). Spearman's rank correlation was used for statistical analysis.

Figure 7. IL-10-producing B and CD4$^+$ T cells revealed by mass cytometry. (**A**) IL-10$^+$ cells were manually gated using Flowjo. Data from one representative individual is shown. (**B**) First HSNE level embedding of total IL-10$^+$ cells, clustered on surface markers. (**C**) Density features of IL-10$^+$. (**D**) The major immune cell subsets producing IL-10, annotated on the basis of lineage marker expression (*See Fig. S4*). (**E**) Data level embedding of IL-10$^+$ B cells and the cluster partitions using GMS clustering (lower right panel). (**F**) Relative composition of IL-10$^+$ B cells, comparing EU (n=10) and ID Pre (n=10). Below, density features of IL-10$^+$ B cells are shown. (**G**) First level HSNE embedding of IL-10$^+$CD4$^+$ landmarks selected in Fig. 7D and clustered on cytokines. Four IL-4/5/13$^+$ clusters were identified as indicated in the right panel showing the cluster partitions. (**H**) Histograms showing the median signal intensity (MSI) distribution of cytokines for the four clusters identified in Fig. 7G. (**I**) Frequency of cluster 1, co-expressing IL-4/5/13 and IL-10 (identified in Fig. 7G), relative to total IL-10-producing CD4$^+$ T cells.

Differences between EU and ID Pre were tested with Student's *t* test, whereas differences between ID Pre and ID Post (n=10) were assessed using paired *t* tests. **P* <0.05; ***P* <0.01.

Figure 8. The immune profile of urban Indonesians is more similar to Europeans than rural Indonesians (**A**) Frequency of Th2 cells relative to $CD4^+$ T cells. Differences between EU (n=8), Indonesians from urban settings without helminth infections (urban ID, n=8) and rural Indonesians infected with helminths (rural ID, n=8) were tested with ANOVA followed by Tukey's post-test. ***P* <0.01, ****P* <0.001. (**B**) Third HSNE level embedding of the Th2 cells and theirdensity features . (**C**) Frequency of $CD161^+CD27^-$ cells within Th2 cells. **P* <0.05, ***P* <0.01. (**D**) Data level embedding of ILC2s. The upper right panel shows the cluster partitions using GMS clustering, whereas the other panels show the expression of KRLG1, CCR6 and CD45RA. Right panel shows the frequency of $CCR6^-KLRG1^+$ cells within ILC2s. **P* <0.05, ***P* <0.01. (**E**) Frequency of IL4/5/13 producing cells within $CD4^+$ T cells. **P <.01, ****P* <0.001. (**F**) Frequency of IL4/5/13 producing cells within ILC2s. **P* <0.05. (**G**) Frequency of $CD161^+$ (left panel) and CTLA-4^+ (right panel) cells within Tregs. **P* <0.05, ***P* <0.01, ****P* <0.001. (**H**) Data level embedding of IL-10^+ B cells and the cluster partitions using GMS clustering (lower right panel), whereas the other right panels show the expression of CD11c, CD38 and the density features in left panels. (**I**) Frequency of $CD11c^+$ cells within IL10-producing B cells. ***P* <0.01.

References and Notes

1. M. Patel, A. L. Shane, U. D. Parashar, B. Jiang, J. R. Gentsch, R. I. Glass, Oral rotavirus vaccines: how well will they work where they are needed most? *J Infect Dis* **200 Suppl 1**, S39-48 (2009); published online EpubNov 1 (10.1086/605035).
2. M. K. Lalor, S. Floyd, P. Gorak-Stolinska, A. Ben-Smith, R. E. Weir, S. G. Smith, M. J. Newport, R. Blitz, H. Mvula, K. Branson, N. McGrath, A. C. Crampin, P. E. Fine, H. M. Dockrell, BCG vaccination induces different cytokine profiles following infant BCG vaccination in the UK and Malawi. *J Infect Dis* **204**, 1075-1085 (2011); published online EpubOct 1 (10.1093/infdis/jir515).
3. P. Brodin, V. Jojic, T. Gao, S. Bhattacharya, C. J. Angel, D. Furman, S. Shen-Orr, C. L. Dekker, G. E. Swan, A. J. Butte, H. T. Maecker, M. M. Davis, Variation in the human immune system is largely driven by non-heritable influences. *Cell* **160**, 37-47 (2015); published online EpubJan 15 (10.1016/j.cell.2014.12.020).
4. Y. Idaghdour, J. D. Storey, S. J. Jadallah, G. Gibson, A genome-wide gene expression signature of environmental geography in leukocytes of Moroccan Amazighs. *PLoS Genet* **4**, e1000052 (2008); published online EpubApr 11 (10.1371/journal.pgen.1000052).
5. P. J. Hotez, P. J. Brindley, J. M. Bethony, C. H. King, E. J. Pearce, J. Jacobson, Helminth infections: the great neglected tropical diseases. *J Clin Invest* **118**, 1311-1321 (2008); published online EpubApr (10.1172/JCI34261).
6. R. M. Maizels, M. Yazdanbakhsh, Immune regulation by helminth parasites: cellular and molecular mechanisms. *Nat Rev Immunol* **3**, 733-744 (2003); published online EpubSep (10.1038/nri1183).
7. D. R. Neill, S. H. Wong, A. Bellosi, R. J. Flynn, M. Daly, T. K. Langford, C. Bucks, C. M. Kane, P. G. Fallon, R. Pannell, H. E. Jolin, A. N. McKenzie, Nuocytes represent a new innate effector leukocyte that mediates type-2 immunity. *Nature* **464**, 1367-1370 (2010); published online EpubApr 29 (10.1038/nature08900).
8. K. Moro, T. Yamada, M. Tanabe, T. Takeuchi, T. Ikawa, H. Kawamoto, J. Furusawa, M. Ohtani, H. Fujii, S. Koyasu, Innate production of T(H)2 cytokines by adipose tissue-associated c-Kit(+)Sca-1(+) lymphoid cells. *Nature* **463**, 540-544 (2010); published online EpubJan 28 (10.1038/nature08636).
9. A. E. Price, H. E. Liang, B. M. Sullivan, R. L. Reinhardt, C. J. Eisley, D. J. Erle, R. M. Locksley, Systemically dispersed innate IL-13-expressing cells in type 2 immunity. *Proc Natl Acad Sci U S A* **107**, 11489-11494 (2010); published online EpubJun 22 (10.1073/pnas.1003988107).
10. Y. Simoni, E. W. Newell, Dissecting human ILC heterogeneity: more than just three subsets. *Immunology* **153**, 297-303 (2018); published online EpubMar (10.1111/imm.12862).
11. N. L. Harris, P. Loke, Recent Advances in Type-2-Cell-Mediated Immunity: Insights from Helminth Infection. *Immunity* **47**, 1024-1036 (2017); published online EpubDec 19 (10.1016/j.immuni.2017.11.015).
12. J. E. Allen, T. E. Sutherland, Host protective roles of type 2 immunity: parasite killing and tissue repair, flip sides of the same coin. *Semin Immunol* **26**, 329-340 (2014); published online EpubAug (10.1016/j.smim.2014.06.003).
13. C. M. Lloyd, R. J. Snelgrove, Type 2 immunity: Expanding our view. *Sci Immunol* **3**, (2018); published online EpubJul 6 (10.1126/sciimmunol.aat1604).
14. B. Pulendran, D. Artis, New paradigms in type 2 immunity. *Science* **337**, 431-435 (2012); published online EpubJul 27 (10.1126/science.1221064).
15. R. M. Maizels, K. A. Smith, Regulatory T cells in infection. *Adv Immunol* **112**, 73-136 (2011)10.1016/B978-0-12-387827-4.00003-6).
16. S. Metenou, T. B. Nutman, Regulatory T cell subsets in filarial infection and their function. *Front Immunol* **4**, 305 (2013); published online EpubSep 30 (10.3389/fimmu.2013.00305).
17. K. Watanabe, P. N. Mwinzi, C. L. Black, E. M. Muok, D. M. Karanja, W. E. Secor, D. G. Colley, T regulatory cell levels decrease in people infected with Schistosoma mansoni on effective treatment. *Am J Trop Med Hyg* **77**, 676-682 (2007); published online EpubOct (
18. L. J. Wammes, F. Hamid, A. E. Wiria, B. de Gier, E. Sartono, R. M. Maizels, A. J. Luty, Y. Fillie, G. T. Brice, T. Supali, H. H. Smits, M. Yazdanbakhsh, Regulatory T cells in human geohelminth infection suppress immune responses to BCG and Plasmodium falciparum. *European journal of immunology* **40**, 437-442 (2010); published online EpubFeb (10.1002/eji.200939699).
19. E. van Riet, F. C. Hartgers, M. Yazdanbakhsh, Chronic helminth infections induce immunomodulation: consequences and mechanisms. *Immunobiology* **212**, 475-490 (2007)10.1016/j.imbio.2007.03.009).

20. S. Sakaguchi, M. Miyara, C. M. Costantino, D. A. Hafler, FOXP3+ regulatory T cells in the human immune system. *Nat Rev Immunol* **10**, 490-500 (2010); published online EpubJul (10.1038/nri2785).
21. L. J. Wammes, F. Hamid, A. E. Wiria, L. May, M. M. Kaisar, M. A. Prasetyani-Gieseler, Y. Djuardi, H. Wibowo, Y. C. Kruize, J. J. Verweij, S. E. de Jong, R. Tsonaka, J. J. Houwing-Duistermaat, E. Sartono, A. J. Luty, T. Supali, M. Yazdanbakhsh, Community deworming alleviates geohelminth-induced immune hyporesponsiveness. *Proc Natl Acad Sci U S A* **113**, 12526-12531 (2016); published online EpubNov 1 (10.1073/pnas.1604570113).
22. M. H. Spitzer, G. P. Nolan, Mass Cytometry: Single Cells, Many Features. *Cell* **165**, 780-791 (2016); published online EpubMay 5 (10.1016/j.cell.2016.04.019).
23. L. van der Maaten, G. Hinton, Visualizing Data using t-SNE. *J Mach Learn Res* **9**, 2579-2605 (2008); published online EpubNov (
24. H. J. McInnes L, UMAP: Uniform Manifold Approximation and Projection for Dimension Reduction. *https://arxiv.org/pdf/1802.03426.pdf*, (2018).
25. N. Pezzotti, T. Hollt, B. Lelieveldt, E. Eisemann, A. Vilanova, Hierarchical Stochastic Neighbor Embedding. *Comput Graph Forum* **35**, 21-30 (2016); published online EpubJun (10.1111/cgf.12878).
26. V. van Unen, T. Hollt, N. Pezzotti, N. Li, M. J. T. Reinders, E. Eisemann, F. Koning, A. Vilanova, B. P. F. Lelieveldt, Visual analysis of mass cytometry data by hierarchical stochastic neighbour embedding reveals rare cell types. *Nat Commun* **8**, 1740 (2017); published online EpubNov 23 (10.1038/s41467-017-01689-9).
27. L. Cosmi, F. Annunziato, M. I. G. Galli, R. M. E. Maggi, K. Nagata, S. Romagnani, CRTH2 is the most reliable marker for the detection of circulating human type 2 Th and type 2 T cytotoxic cells in health and disease. *Eur J Immunol* **30**, 2972-2979 (2000); published online EpubOct (10.1002/1521-4141(200010)30:10<2972::AID-IMMU2972>3.0.CO;2-#).
28. Y. D. Mahnke, T. M. Brodie, F. Sallusto, M. Roederer, E. Lugli, The who's who of T-cell differentiation: human memory T-cell subsets. *European journal of immunology* **43**, 2797-2809 (2013); published online EpubNov (10.1002/eji.201343751).
29. A. Schiott, M. Lindstedt, B. Johansson-Lindbom, E. Roggen, C. A. Borrebaeck, CD27- CD4+ memory T cells define a differentiated memory population at both the functional and transcriptional levels. *Immunology* **113**, 363-370 (2004); published online EpubNov (10.1111/j.1365-2567.2004.01974.x).
30. S. M. Henson, A. N. Akbar, KLRG1--more than a marker for T cell senescence. *Age (Dordr)* **31**, 285-291 (2009); published online EpubDec (10.1007/s11357-009-9100-9).
31. W. Zheng, R. A. Flavell, The transcription factor GATA-3 is necessary and sufficient for Th2 cytokine gene expression in CD4 T cells. *Cell* **89**, 587-596 (1997); published online EpubMay 16 (
32. E. MacLean Scott, L. A. Solomon, C. Davidson, J. Storie, N. S. Palikhe, L. Cameron, Activation of Th2 cells downregulates CRTh2 through an NFAT1 mediated mechanism. *PLoS One* **13**, e0199156 (2018)10.1371/journal.pone.0199156).
33. Y. Simoni, M. Fehlings, H. N. Kloverpris, N. McGovern, S. L. Koo, C. Y. Loh, S. Lim, A. Kurioka, J. R. Fergusson, C. L. Tang, M. H. Kam, K. Dennis, T. K. H. Lim, A. C. Y. Fui, C. W. Hoong, J. K. Y. Chan, M. Curotto de Lafaille, S. Narayanan, S. Baig, M. Shabeer, S. E. S. Toh, H. K. K. Tan, R. Anicete, E. H. Tan, A. Takano, P. Klenerman, A. Leslie, D. S. W. Tan, I. B. Tan, F. Ginhoux, E. W. Newell, Human Innate Lymphoid Cell Subsets Possess Tissue-Type Based Heterogeneity in Phenotype and Frequency. *Immunity* **46**, 148-161 (2017); published online EpubJan 17 (10.1016/j.immuni.2016.11.005).
34. A. I. Lim, S. Menegatti, J. Bustamante, L. Le Bourhis, M. Allez, L. Rogge, J. L. Casanova, H. Yssel, J. P. Di Santo, IL-12 drives functional plasticity of human group 2 innate lymphoid cells. *J Exp Med* **213**, 569-583 (2016); published online EpubApr 4 (10.1084/jem.20151750).
35. T. Ito, W. F. t. Carson, K. A. Cavassani, J. M. Connett, S. L. Kunkel, CCR6 as a mediator of immunity in the lung and gut. *Exp Cell Res* **317**, 613-619 (2011); published online EpubMar 10 (10.1016/j.yexcr.2010.12.018).
36. H. C. Jeffery, P. McDowell, P. Lutz, R. E. Wawman, S. Roberts, C. Bagnall, J. Birtwistle, D. H. Adams, Y. H. Oo, Human intrahepatic ILC2 are IL-13positive amphiregulinpositive and their frequency correlates with model of end stage liver disease score. *PLoS One* **12**, e0188649 (2017)10.1371/journal.pone.0188649).
37. K. Wing, Y. Onishi, P. Prieto-Martin, T. Yamaguchi, M. Miyara, Z. Fehervari, T. Nomura, S. Sakaguchi, CTLA-4 control over Foxp3+ regulatory T cell function. *Science* **322**, 271-275 (2008); published online EpubOct 10 (10.1126/science.1160062).
38. G. A. M. Povoleri, E. Nova-Lamperti, C. Scotta, G. Fanelli, Y. C. Chen, P. D. Becker, D. Boardman, B. Costantini, M. Romano, P. Pavlidis, R. McGregor, E. Pantazi, D. Chauss, H. W. Sun, H. Y. Shih, D. J.

Cousins, N. Cooper, N. Powell, C. Kemper, M. Pirooznia, A. Laurence, S. Kordasti, M. Kazemian, G. Lombardi, B. Afzali, Human retinoic acid-regulated CD161(+) regulatory T cells support wound repair in intestinal mucosa. *Nat Immunol* **19**, 1403-1414 (2018); published online EpubDec (10.1038/s41590-018-0230-z).

39. R. A. Seder, G. G. Le Gros, The functional role of CD8+ T helper type 2 cells. *J Exp Med* **181**, 5-7 (1995); published online EpubJan 1 (
40. B. Hilvering, T. S. C. Hinks, L. Stoger, E. Marchi, M. Salimi, R. Shrimanker, W. Liu, W. Chen, J. Luo, S. Go, T. Powell, J. Cane, S. Thulborn, A. Kurioka, T. Leng, J. Matthews, C. Connolly, C. Borg, M. Bafadhel, C. B. Willberg, A. Ramasamy, R. Djukanovic, G. Ogg, I. D. Pavord, P. Klenerman, L. Xue, Synergistic activation of pro-inflammatory type-2 CD8(+) T lymphocytes by lipid mediators in severe eosinophilic asthma. *Mucosal Immunol*, (2018); published online EpubJun 15 (10.1038/s41385-018-0049-9).
41. A. Hardjanti, P. Rachmawati, T. Cresnaulan Desiyanti, R. Fauzi Rahman, Y. Wahyudi, Y. Intan Farellina, Prevalensi dan Tingkat Infeksi Soil Transmitted Helminths Dihubungkan dengan Golongan Usia dan Jenis Kelamin pada 5 Sekolah Dasar. *Majalah Kesehatan Pharmamedika* **9**, 086 (2018); published online Epub11/26 (10.33476/mkp.v9i2.680).
42. K. de Ruiter, D. L. Tahapary, E. Sartono, P. Soewondo, T. Supali, J. W. A. Smit, M. Yazdanbakhsh, Helminths, hygiene hypothesis and type 2 diabetes. *Parasite Immunol* **39**, (2017); published online EpubMay (10.1111/pim.12404).
43. A. Boyd, J. M. Ribeiro, T. B. Nutman, Human CD117 (cKit)+ innate lymphoid cells have a discrete transcriptional profile at homeostasis and are expanded during filarial infection. *PLoS One* **9**, e108649 (2014)10.1371/journal.pone.0108649).
44. N. Nausch, L. J. Appleby, A. M. Sparks, N. Midzi, T. Mduluza, F. Mutapi, Group 2 innate lymphoid cell proportions are diminished in young helminth infected children and restored by curative anti-helminthic treatment. *PLoS Negl Trop Dis* **9**, e0003627 (2015); published online EpubMar (10.1371/journal.pntd.0003627).
45. J. M. Mjosberg, S. Trifari, N. K. Crellin, C. P. Peters, C. M. van Drunen, B. Piet, W. J. Fokkens, T. Cupedo, H. Spits, Human IL-25- and IL-33-responsive type 2 innate lymphoid cells are defined by expression of CRTH2 and CD161. *Nat Immunol* **12**, 1055-1062 (2011); published online EpubSep 11 (10.1038/ni.2104).
46. H. Spits, D. Artis, M. Colonna, A. Diefenbach, J. P. Di Santo, G. Eberl, S. Koyasu, R. M. Locksley, A. N. McKenzie, R. E. Mebius, F. Powrie, E. Vivier, Innate lymphoid cells--a proposal for uniform nomenclature. *Nat Rev Immunol* **13**, 145-149 (2013); published online EpubFeb (10.1038/nri3365).
47. A. I. Lim, Y. Li, S. Lopez-Lastra, R. Stadhouders, F. Paul, A. Casrouge, N. Serafini, A. Puel, J. Bustamante, L. Surace, G. Masse-Ranson, E. David, H. Strick-Marchand, L. Le Bourhis, R. Cocchi, D. Topazio, P. Graziano, L. A. Muscarella, L. Rogge, X. Norel, J. M. Sallenave, M. Allez, T. Graf, R. W. Hendriks, J. L. Casanova, I. Amit, H. Yssel, J. P. Di Santo, Systemic Human ILC Precursors Provide a Substrate for Tissue ILC Differentiation. *Cell* **168**, 1086-1100 e1010 (2017); published online EpubMar 9 (10.1016/j.cell.2017.02.021).
48. A. Mitson-Salazar, Y. Yin, D. L. Wansley, M. Young, H. Bolan, S. Arceo, N. Ho, C. Koh, J. D. Milner, K. D. Stone, S. A. Wank, C. Prussin, Hematopoietic prostaglandin D synthase defines a proeosinophilic pathogenic effector human T(H)2 cell subpopulation with enhanced function. *J Allergy Clin Immunol* **137**, 907-918 e909 (2016); published online EpubMar (10.1016/j.jaci.2015.08.007).
49. A. Mitson-Salazar, C. Prussin, Pathogenic Effector Th2 Cells in Allergic Eosinophilic Inflammatory Disease. *Front Med (Lausanne)* **4**, 165 (2017)10.3389/fmed.2017.00165).
50. F. Hamid, S. A. Versteeg, A. E. Wiria, L. J. Wammes, S. Wahyuni, T. Supali, E. Sartono, R. van Ree, M. Yazdanbakhsh, Molecular diagnostics and lack of clinical allergy in helminth-endemic areas in Indonesia. *J Allergy Clin Immunol* **140**, 1196-1199 e1196 (2017); published online EpubOct (10.1016/j.jaci.2017.04.040).
51. C. Baecher-Allan, E. Wolf, D. A. Hafler, MHC class II expression identifies functionally distinct human regulatory T cells. *J Immunol* **176**, 4622-4631 (2006); published online EpubApr 15 (
52. T. Ito, S. Hanabuchi, Y. H. Wang, W. R. Park, K. Arima, L. Bover, F. X. Qin, M. Gilliet, Y. J. Liu, Two functional subsets of FOXP3+ regulatory T cells in human thymus and periphery. *Immunity* **28**, 870-880 (2008); published online EpubJun (10.1016/j.immuni.2008.03.018).
53. D. T. Patton, M. D. Wilson, W. C. Rowan, D. R. Soond, K. Okkenhaug, The PI3K p110delta regulates expression of CD38 on regulatory T cells. *PLoS One* **6**, e17359 (2011); published online EpubMar 1 (10.1371/journal.pone.0017359).

54. D. A. Ferrick, M. D. Schrenzel, T. Mulvania, B. Hsieh, W. G. Ferlin, H. Lepper, Differential production of interferon-gamma and interleukin-4 in response to Th1- and Th2-stimulating pathogens by gamma delta T cells in vivo. *Nature* **373**, 255-257 (1995); published online EpubJan 19 (10.1038/373255a0).
55. K. Inagaki-Ohara, Y. Sakamoto, T. Dohi, A. L. Smith, gammadelta T cells play a protective role during infection with Nippostrongylus brasiliensis by promoting goblet cell function in the small intestine. *Immunology* **134**, 448-458 (2011); published online EpubDec (10.1111/j.1365-2567.2011.03503.x).
56. C. Zuany-Amorim, C. Ruffie, S. Haile, B. B. Vargaftig, P. Pereira, M. Pretolani, Requirement for gammadelta T cells in allergic airway inflammation. *Science* **280**, 1265-1267 (1998); published online EpubMay 22 (
57. F. Spinozzi, E. Agea, O. Bistoni, N. Forenza, A. Monaco, G. Bassotti, I. Nicoletti, C. Riccardi, F. Grignani, A. Bertotto, Increased allergen-specific, steroid-sensitive gamma delta T cells in bronchoalveolar lavage fluid from patients with asthma. *Ann Intern Med* **124**, 223-227 (1996); published online EpubJan 15 (
58. N. Krug, V. J. Erpenbeck, K. Balke, J. Petschallies, T. Tschernig, J. M. Hohlfeld, H. Fabel, Cytokine profile of bronchoalveolar lavage-derived CD4(+), CD8(+), and gammadelta T cells in people with asthma after segmental allergen challenge. *Am J Respir Cell Mol Biol* **25**, 125-131 (2001); published online EpubJul (10.1165/ajrcmb.25.1.4194).
59. K. W. Dantzler, P. Jagannathan, gammadelta T Cells in Antimalarial Immunity: New Insights Into Their Diverse Functions in Protection and Tolerance. *Front Immunol* **9**, 2445 (2018)10.3389/fimmu.2018.02445).
60. S. J. Lalor, R. M. McLoughlin, Memory gammadelta T Cells-Newly Appreciated Protagonists in Infection and Immunity. *Trends Immunol* **37**, 690-702 (2016); published online EpubOct (10.1016/j.it.2016.07.006).
61. C. Mauri, M. Menon, The expanding family of regulatory B cells. *Int Immunol* **27**, 479-486 (2015); published online EpubOct (10.1093/intimm/dxv038).
62. J. L. Karnell, V. Kumar, J. Wang, S. Wang, E. Voynova, R. Ettinger, Role of CD11c(+) T-bet(+) B cells in human health and disease. *Cell Immunol* **321**, 40-45 (2017); published online EpubNov (10.1016/j.cellimm.2017.05.008).
63. G. M. Winslow, A. M. Papillion, K. J. Kenderes, R. C. Levack, CD11c+ T-bet+ memory B cells: Immune maintenance during chronic infection and inflammation? *Cell Immunol* **321**, 8-17 (2017); published online EpubNov (10.1016/j.cellimm.2017.07.006).
64. D. L. Tahapary, K. de Ruiter, I. Martin, L. van Lieshout, B. Guigas, P. Soewondo, Y. Djuardi, A. E. Wiria, O. A. Mayboroda, J. J. Houwing-Duistermaat, H. Tasman, E. Sartono, M. Yazdanbakhsh, J. W. Smit, T. Supali, Helminth infections and type 2 diabetes: a cluster-randomized placebo controlled SUGARSPIN trial in Nangapanda, Flores, Indonesia. *BMC Infect Dis* **15**, 133 (2015); published online EpubMar 18 (10.1186/s12879-015-0873-4).
65. D. L. Tahapary, K. de Ruiter, I. Martin, E. A. T. Brienen, L. van Lieshout, C. M. Cobbaert, P. Soewondo, Y. Djuardi, A. E. Wiria, J. J. Houwing-Duistermaat, E. Sartono, J. W. A. Smit, M. Yazdanbakhsh, T. Supali, Effect of Anthelmintic Treatment on Insulin Resistance: A Cluster-Randomized, Placebo-Controlled Trial in Indonesia. *Clin Infect Dis* **65**, 764-771 (2017); published online EpubSep 1 (10.1093/cid/cix416).
66. A. E. Wiria, M. A. Prasetyani, F. Hamid, L. J. Wammes, B. Lell, I. Ariawan, H. W. Uh, H. Wibowo, Y. Djuardi, S. Wahyuni, I. Sutanto, L. May, A. J. Luty, J. J. Verweij, E. Sartono, M. Yazdanbakhsh, T. Supali, Does treatment of intestinal helminth infections influence malaria? Background and methodology of a longitudinal study of clinical, parasitological and immunological parameters in Nangapanda, Flores, Indonesia (ImmunoSPIN Study). *BMC Infect Dis* **10**, 77 (2010)10.1186/1471-2334-10-77).
67. T. Hollt, N. Pezzotti, V. van Unen, F. Koning, E. Eisemann, B. Lelieveldt, A. Vilanova, Cytosplore: Interactive Immune Cell Phenotyping for Large Single-Cell Datasets. *Comput Graph Forum* **35**, 171-180 (2016); published online EpubJun (
68. D. Comaniciu, P. Meer, Mean shift: A robust approach toward feature space analysis. *Ieee T Pattern Anal* **24**, 603-619 (2002); published online EpubMay (Doi 10.1109/34.1000236).
69. G. Beyrend, K. A. Stam, T. Hollt, F. Ossendorp, R. Arens, *Cytofast*: A workflow for visual and quantitative analysis of flow and mass cytometry data to discover immune signatures and correlations. *Computational and Structural Biotechnology Journal*, (2018)https://doi.org/10.1016/j.csbj.2018.10.004).

Acknowledgements: We would like to thank the volunteers who participated in this study. We would also like to thank all field workers from Universitas Indonesia and Nangapanda; Yvonne Kruize, Sanne de Jong and Astrid Voskamp for their help with the study. **Funding:** This work was supported by the Royal Netherlands Academy of Arts and Science (KNAW), Ref 57-SPIN3-JRP awarded to J.W.A.S.; Universitas Indonesia, Research Grant BOPTN 2742/H2.R12/HKP.05.00/2013 awarded to T.S. and the European Union's Horizon 2020 research and innovation programme under the Marie Skłodowska-Curie grant agreement No 707404 awarded to S.P.J.. The opinions expressed in this document reflect only the author's view. The European Commission is not responsible for any use that may be made of the information it contains. **Author contributions:** K.R. was in charge of the field study in Indonesia, designed and performed the experiments, analyzed the data and wrote the manuscript. S.P.J. performed experiments, analyzed the data and reviewed the manuscript. D.L.T. was in charge of the field study in Indonesia, involved in setting up the study, treatment and clinical care. K.A.S. provided input for the data analysis and developed the cytofast package in R. M.K. and S.L. performed experiments. V.U. developed the Cytosplore application and reviewed the manuscript. T.H. developed the Cytosplore application. M.M. provided expertise on rural urban comparisons. B.P.F.L. developed the Cytosplore application. F.K. provided consultation with mass cytometry and reviewed the manuscript. E.S. supervised and coordinated the field study. J.W.A.S. Designed the field study and reviewed the manuscript. T.S. supervised and coordinated the field study and reviewed the manuscript. M.Y. conceived and designed the study, supervised the data analysis and writing of the manuscript. All authors revised the final manuscript. **Competing interests**: The authors declare that they have no competing interests. Data and materials availability: All data associated with this study are present in the paper or Supplementary Materials.

Figures

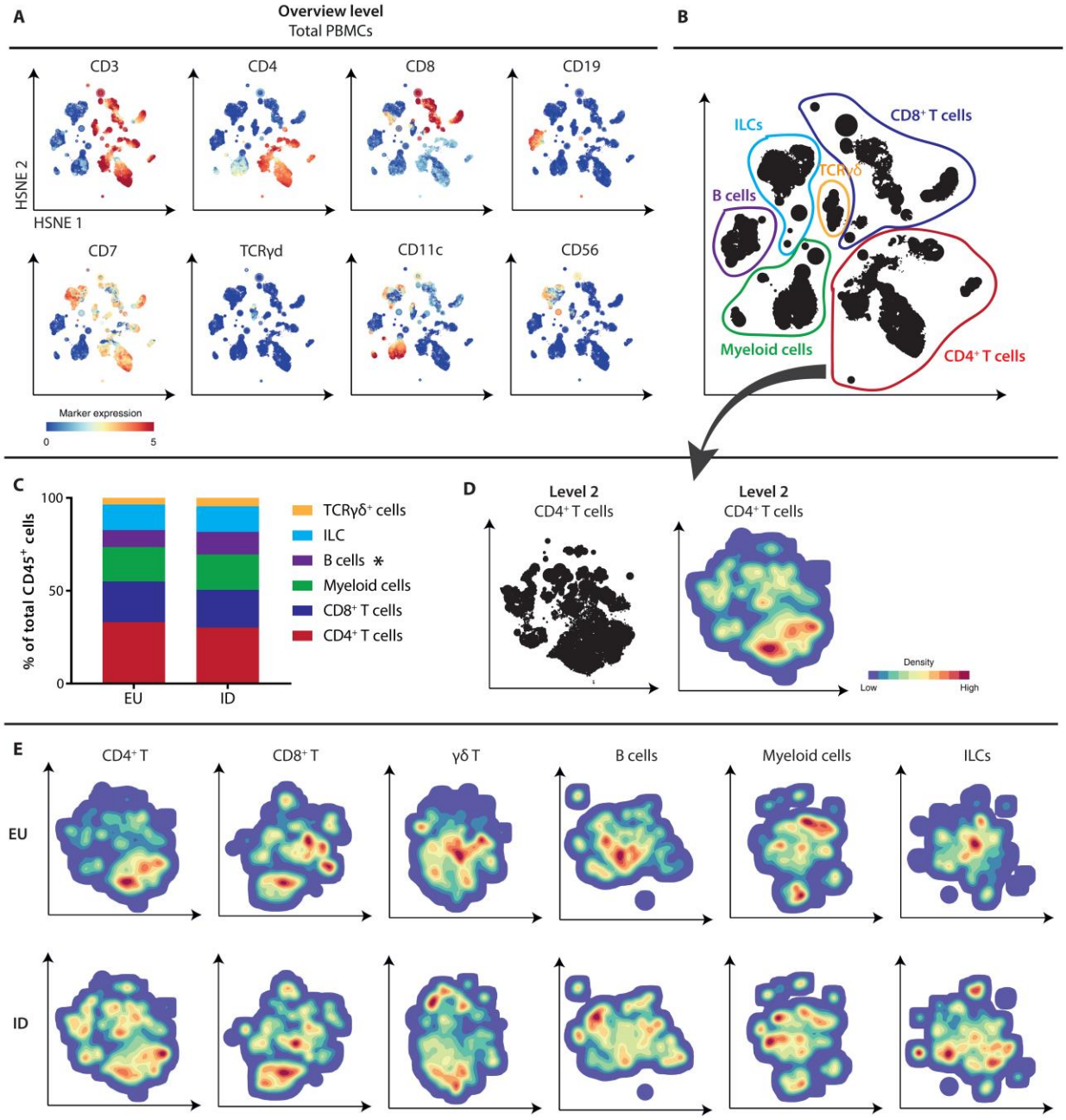

Figure 1

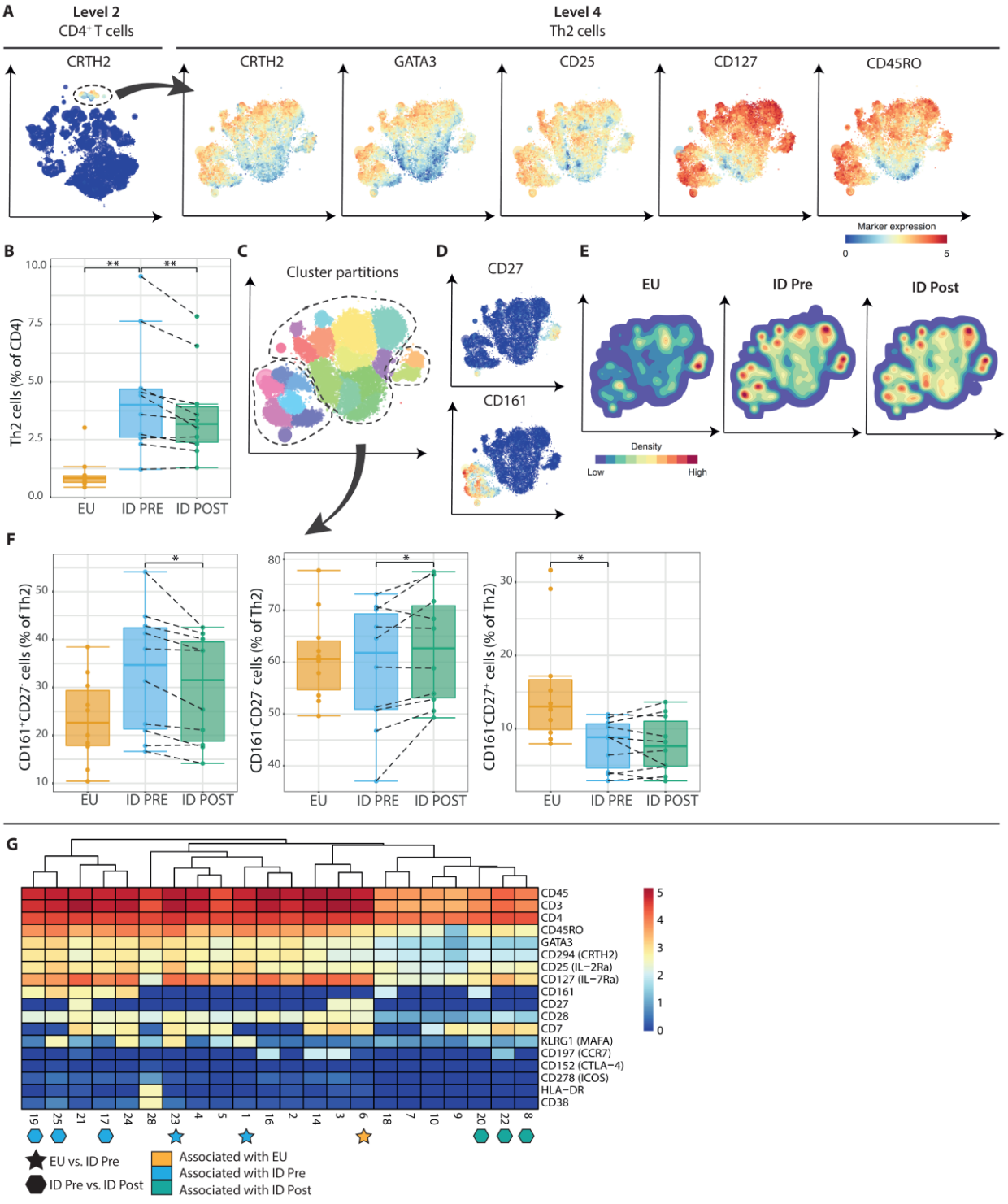
A
Level 2
CD4+ T cells
Level 4
Th2 cells
CRTH2
CRTH2
GATA3
CD25
CD127
CD45RO
Marker expression
0
5
B
Th2 cells (% of CD4)
EU
ID PRE
ID POST
C
Cluster partitions
D
CD27
CD161
E
EU
ID Pre
ID Post
Density
Low
High
F
CD161+CD27- cells (% of Th2)
CD161-CD27- cells (% of Th2)
CD161-CD27+ cells (% of Th2)
G
CD45
CD3
CD4
CD45RO
GATA3
CD294 (CRTH2)
CD25 (IL−2Ra)
CD127 (IL−7Ra)
CD161
CD27
CD28
CD7
KLRG1 (MAFA)
CD197 (CCR7)
CD152 (CTLA−4)
CD278 (ICOS)
HLA−DR
CD38
EU vs. ID Pre
ID Pre vs. ID Post
Associated with EU
Associated with ID Pre
Associated with ID Post

Figure 2

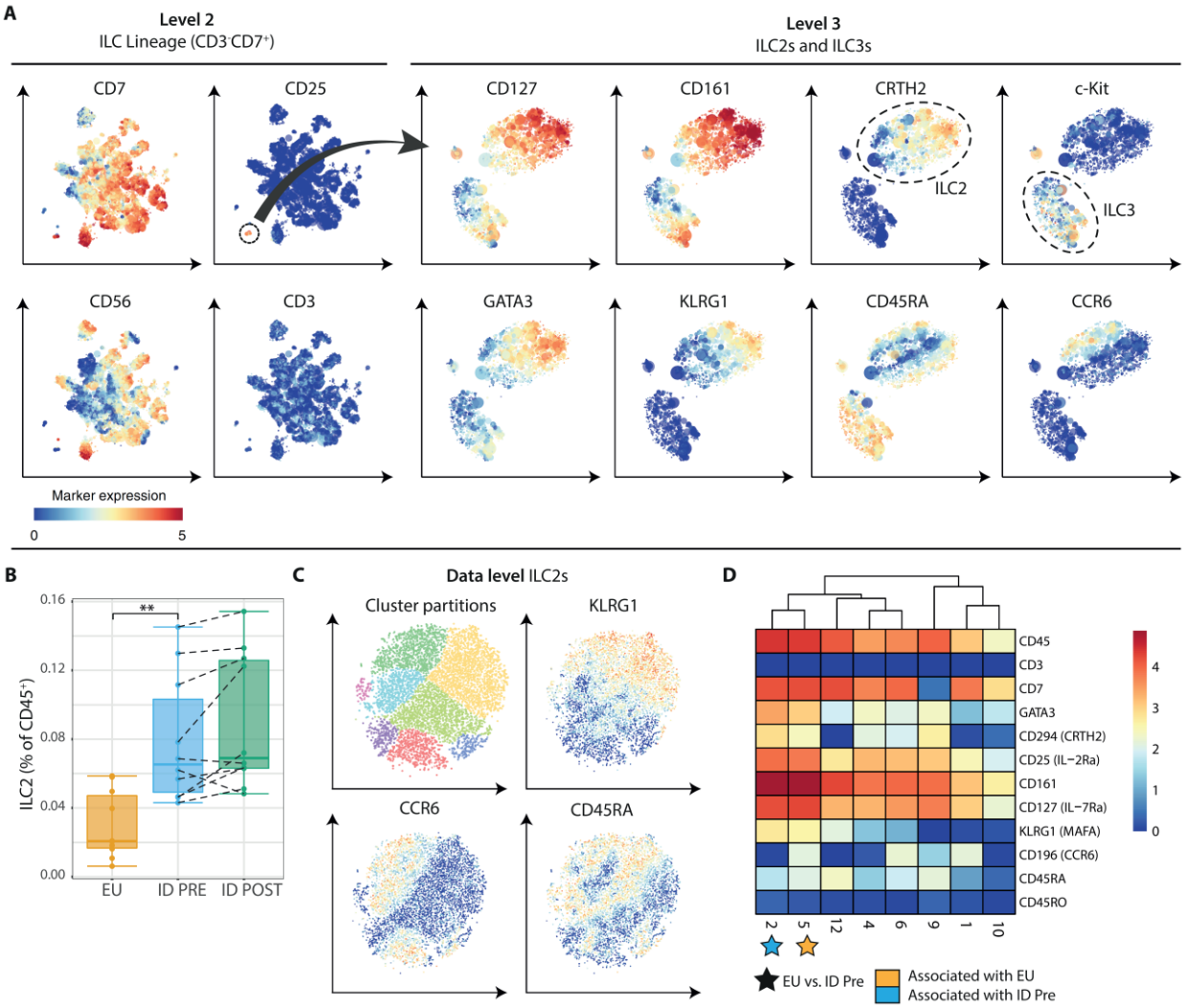
A
Level 2
ILC Lineage (CD3⁻CD7⁺)
Level 3
ILC2s and ILC3s
CD7
CD25
CD127
CD161
CRTH2
c-Kit
ILC2
ILC3
CD56
CD3
GATA3
KLRG1
CD45RA
CCR6
Marker expression
0
5
B
ILC2 (% of CD45⁺)
0.16
0.12
0.08
0.04
0.00
**
EU
ID PRE
ID POST
C
Data level ILC2s
Cluster partitions
KLRG1
CCR6
CD45RA
D
CD45
CD3
CD7
GATA3
CD294 (CRTH2)
CD25 (IL−2Ra)
CD161
CD127 (IL−7Ra)
KLRG1 (MAFA)
CD196 (CCR6)
CD45RA
CD45RO
2
5
12
4
6
9
1
10
4
3
2
1
0
EU vs. ID Pre
Associated with EU
Associated with ID Pre

Figure 3

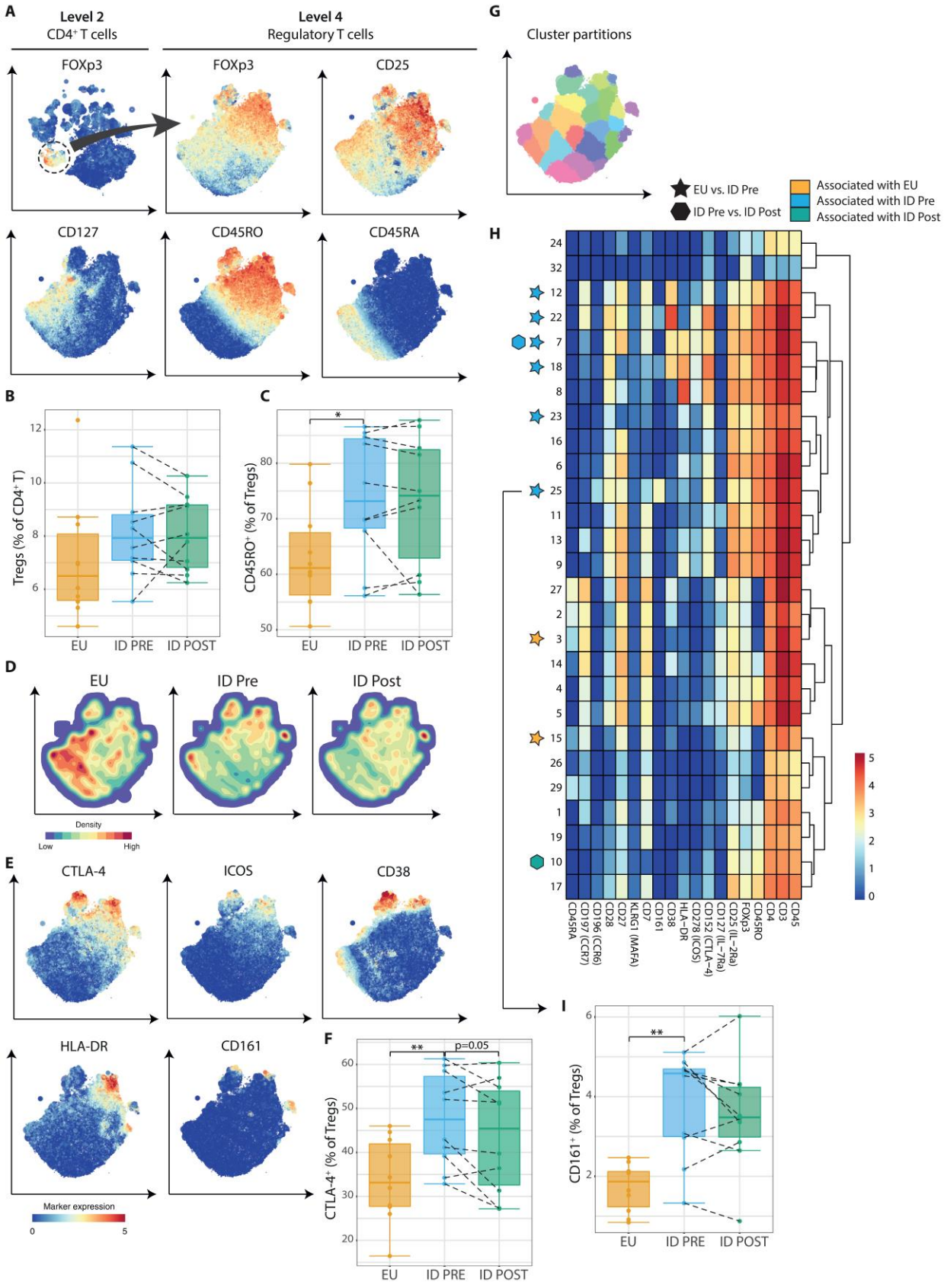
A
Level 2
CD4+ T cells
Level 4
Regulatory T cells
FOXp3
FOXp3
CD25
CD127
CD45RO
CD45RA
B
Tregs (% of CD4+ T)
EU
ID PRE
ID POST
C
CD45RO+ (% of Tregs)
*
EU
ID PRE
ID POST
D
EU
ID Pre
ID Post
Density
Low
High
E
CTLA-4
ICOS
CD38
HLA-DR
CD161
Marker expression
0
5
F
**
p=0.05
CTLA-4+ (% of Tregs)
EU
ID PRE
ID POST
G
Cluster partitions
EU vs. ID Pre
ID Pre vs. ID Post
Associated with EU
Associated with ID Pre
Associated with ID Post
H
CD45RA
CD197 (CCR7)
CD196 (CCR6)
CD28
CD27
KLRG1 (MAFA)
CD7
CD161
CD38
HLA−DR
CD278 (ICOS)
CD152 (CTLA−4)
CD127 (IL−7Rα)
CD25 (IL−2Rα)
FOXp3
CD45RO
CD4
CD3
CD45
I
**
CD161+ (% of Tregs)
EU
ID PRE
ID POST

Figure 4

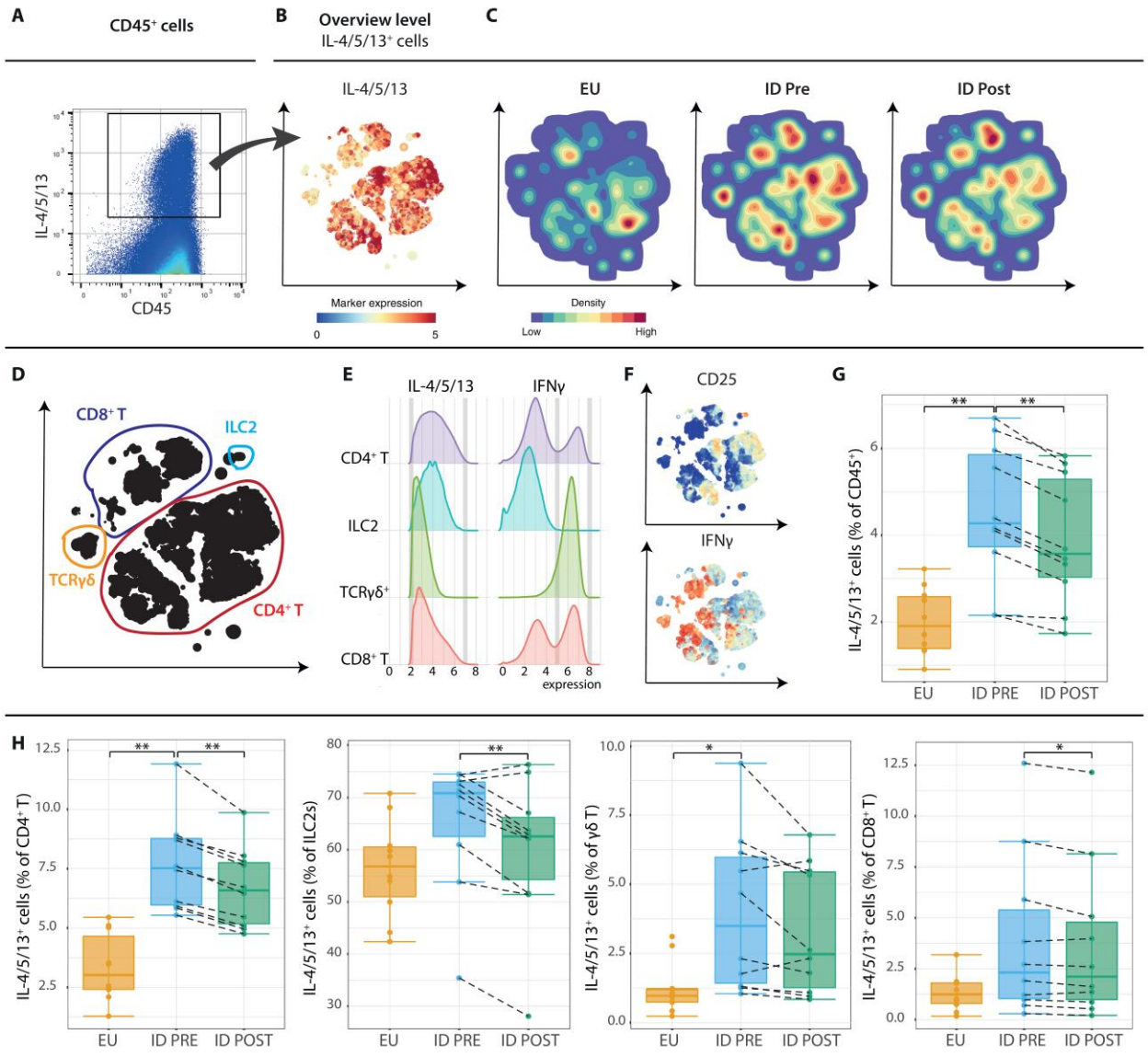
A
CD45⁺ cells
IL-4/5/13
CD45
B
Overview level
IL-4/5/13⁺ cells
IL-4/5/13
Marker expression
0
5
C
EU
ID Pre
ID Post
Density
Low
High
D
CD8⁺ T
ILC2
TCRγδ
CD4⁺ T
E
IL-4/5/13
IFNγ
CD4⁺ T
ILC2
TCRγδ⁺
CD8⁺ T
0 2 4 6 8
0 2 4 6 8
expression
F
CD25
IFNγ
G
IL-4/5/13⁺ cells (% of CD45⁺)
EU
ID PRE
ID POST
H
IL-4/5/13⁺ cells (% of CD4⁺ T)
IL-4/5/13⁺ cells (% of ILC2s)
IL-4/5/13⁺ cells (% of γδ T)
IL-4/5/13⁺ cells (% of CD8⁺ T)
EU
ID PRE
ID POST

Figure 5

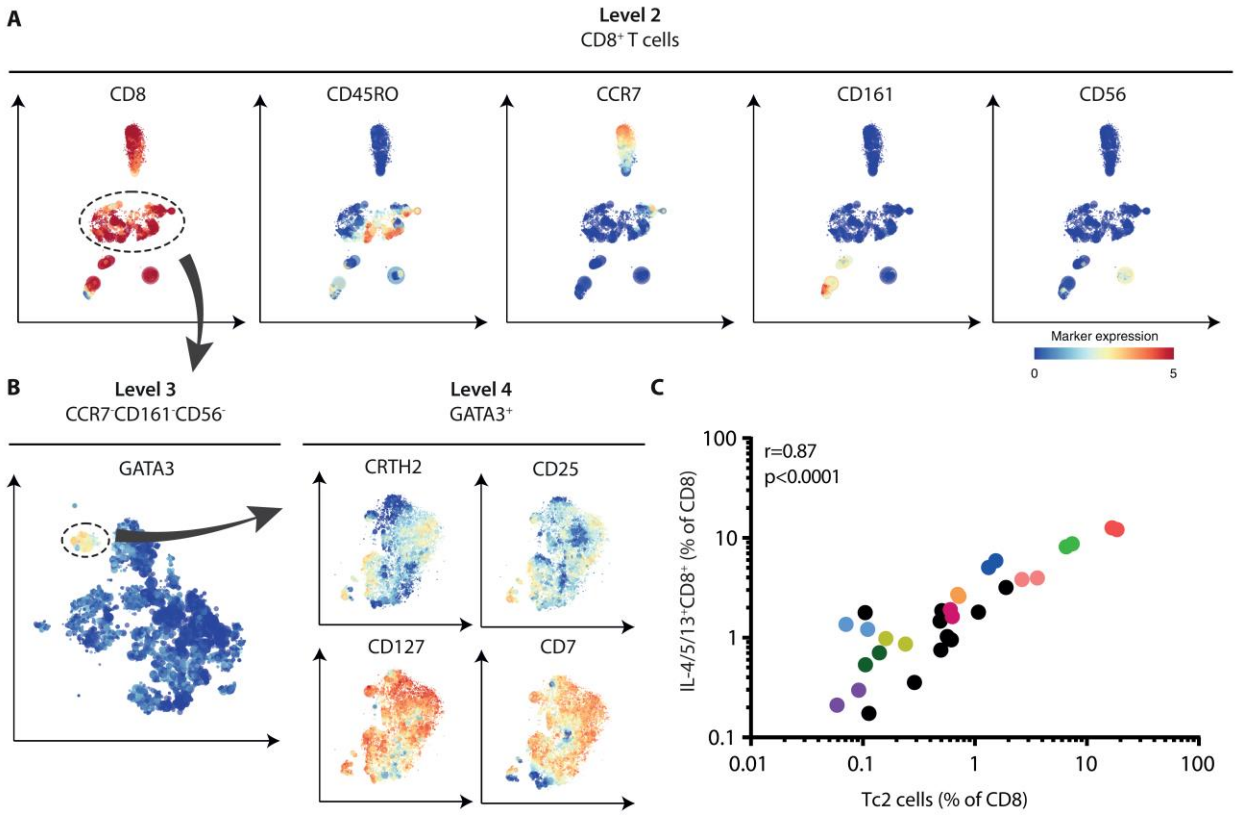
A
Level 2
CD8+ T cells
CD8
CD45RO
CCR7
CD161
CD56
Marker expression
0
5
B
Level 3
CCR7-CD161-CD56-
Level 4
GATA3+
GATA3
CRTH2
CD25
CD127
CD7
C
r=0.87
p<0.0001
IL-4/5/13+CD8+ (% of CD8)
Tc2 cells (% of CD8)
100
10
1
0.1
0.01
0.1
1
10
100

Figure 6

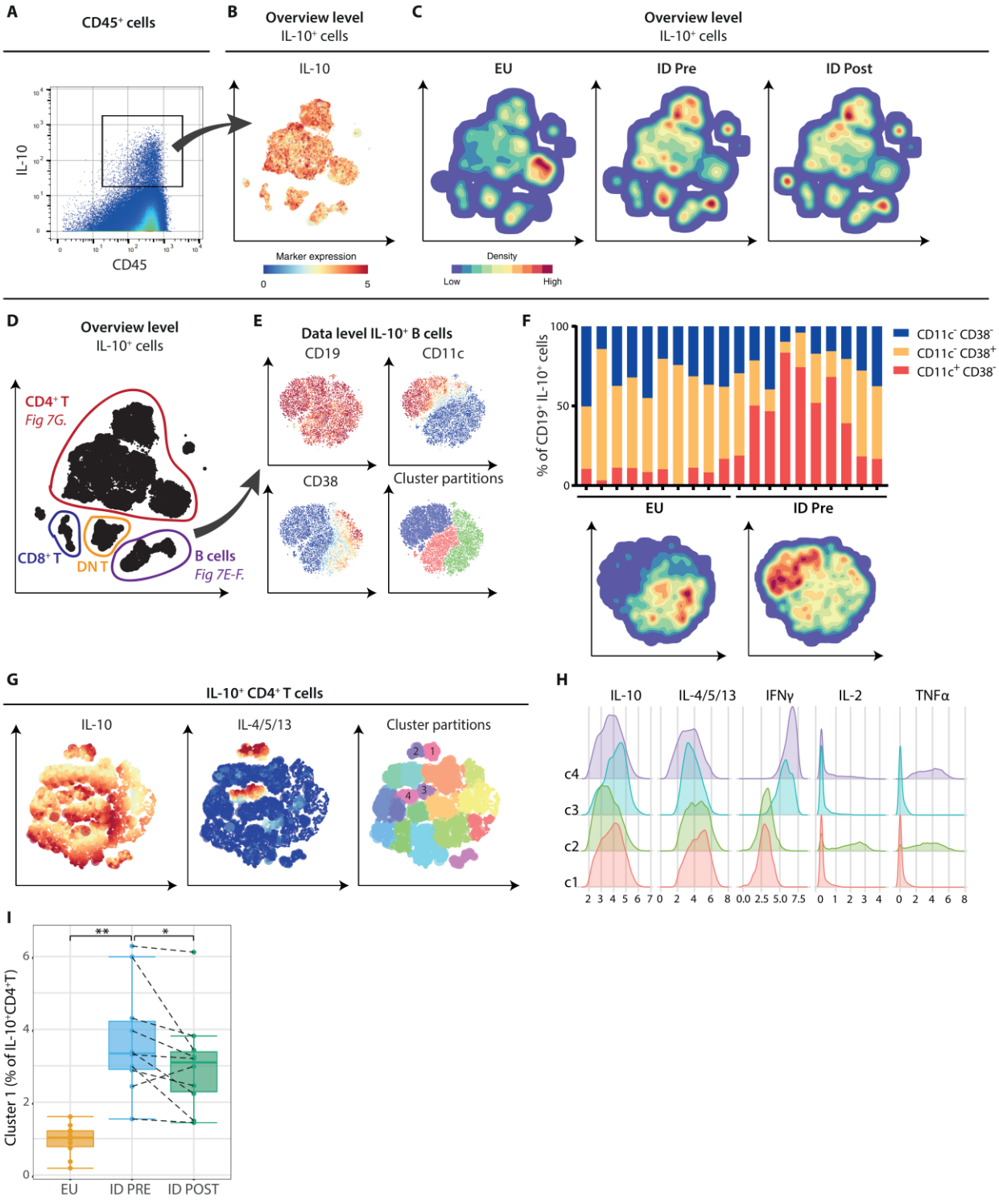
A
CD45⁺ cells
IL-10
CD45
B
Overview level
IL-10⁺ cells
IL-10
Marker expression
0
5
C
Overview level
IL-10⁺ cells
EU
ID Pre
ID Post
Density
Low
High
D
Overview level
IL-10⁺ cells
CD4⁺ T
Fig 7G.
CD8⁺ T
DN T
B cells
Fig 7E-F.
E
Data level IL-10⁺ B cells
CD19
CD11c
CD38
Cluster partitions
F
% of CD19⁺ IL-10⁺ cells
100
50
0
CD11c⁻ CD38⁻
CD11c⁻ CD38⁺
CD11c⁺ CD38⁻
EU
ID Pre
G
IL-10⁺ CD4⁺ T cells
IL-10
IL-4/5/13
Cluster partitions
H
IL-10
IL-4/5/13
IFNγ
IL-2
TNFα
c4
c3
c2
c1
I
Cluster 1 (% of IL-10⁺CD4⁺T)
**
*
EU
ID PRE
ID POST

Figure 7

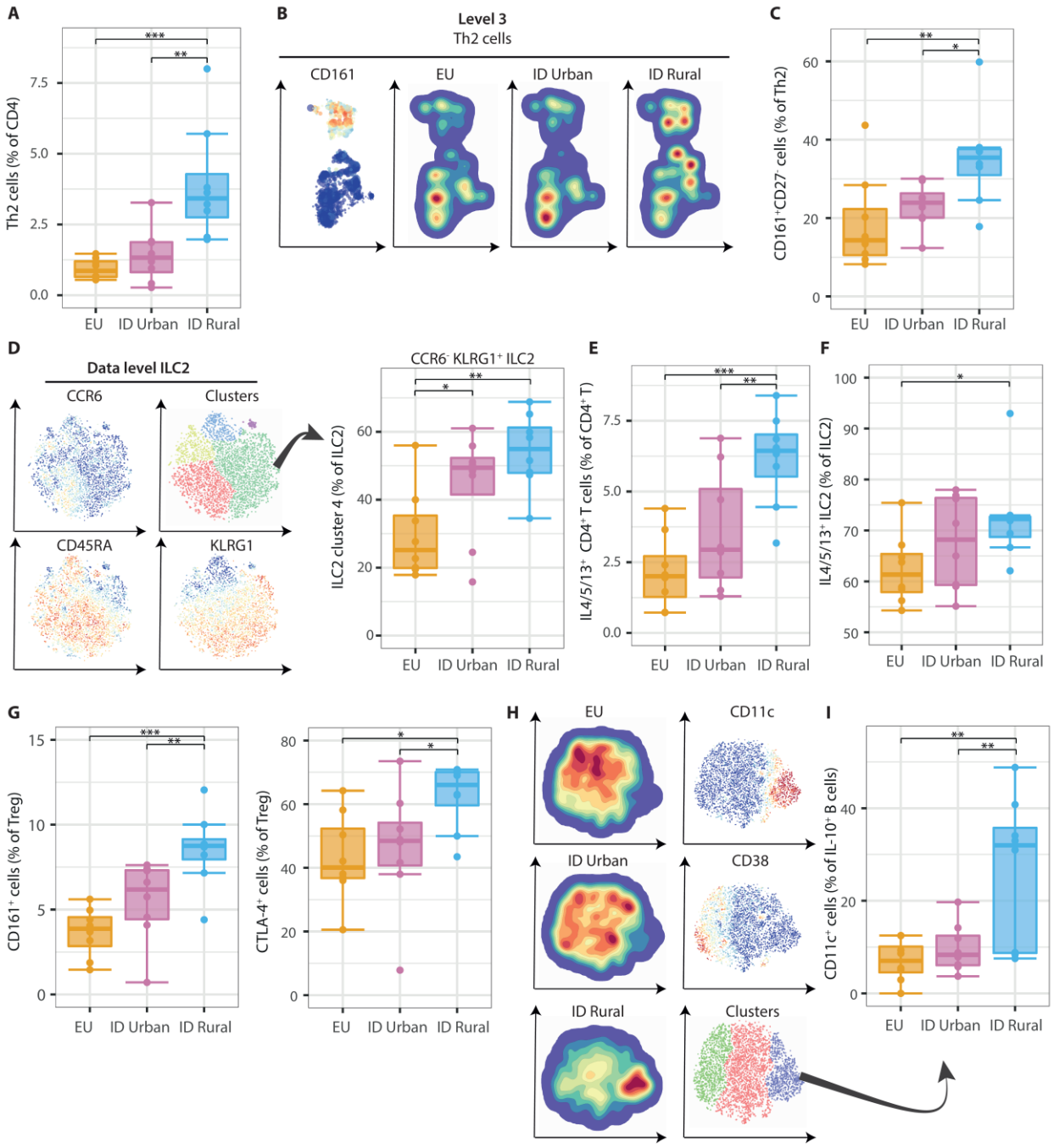
A
Th2 cells (% of CD4)
EU
ID Urban
ID Rural
B
Level 3
Th2 cells
CD161
EU
ID Urban
ID Rural
C
CD161+CD27- cells (% of Th2)
D
Data level ILC2
CCR6
Clusters
CD45RA
KLRG1
CCR6- KLRG1+ ILC2
ILC2 cluster 4 (% of ILC2)
E
IL4/5/13+ CD4+ T cells (% of CD4+ T)
F
IL4/5/13+ ILC2 (% of ILC2)
G
CD161+ cells (% of Treg)
CTLA-4+ cells (% of Treg)
H
EU
CD11c
ID Urban
CD38
ID Rural
Clusters
I
CD11c+ cells (% of IL-10+ B cells)

Figure 8

Supplementary Figures

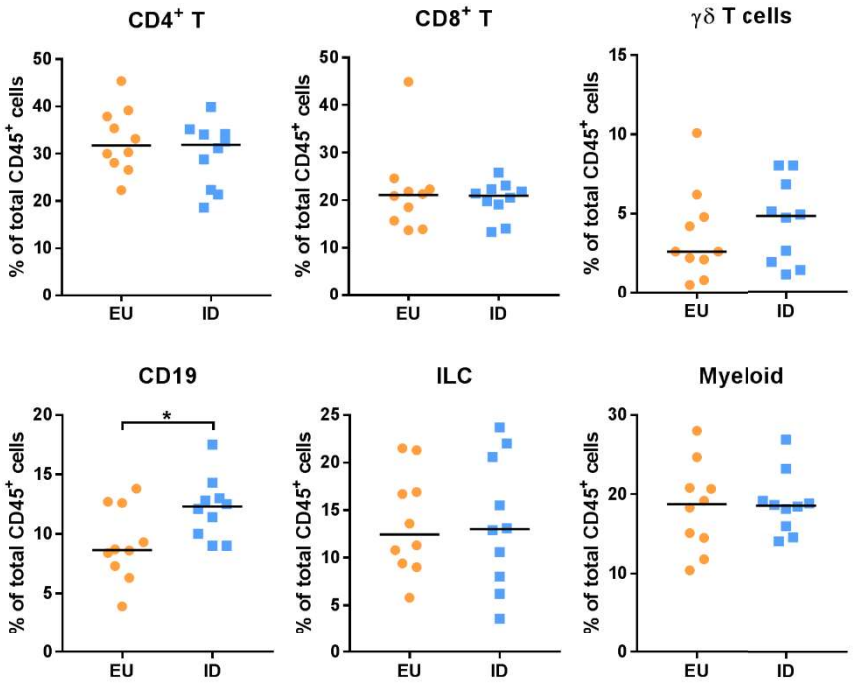

Fig. S1. Lineage frequencies. Scatterplots comparing lineage frequencies of Europeans (EU, n=10) and rural Indonesians (ID, n=10). Median is shown. Differences between EU and ID Pre were tested with Student's t-test. *P <0.05.

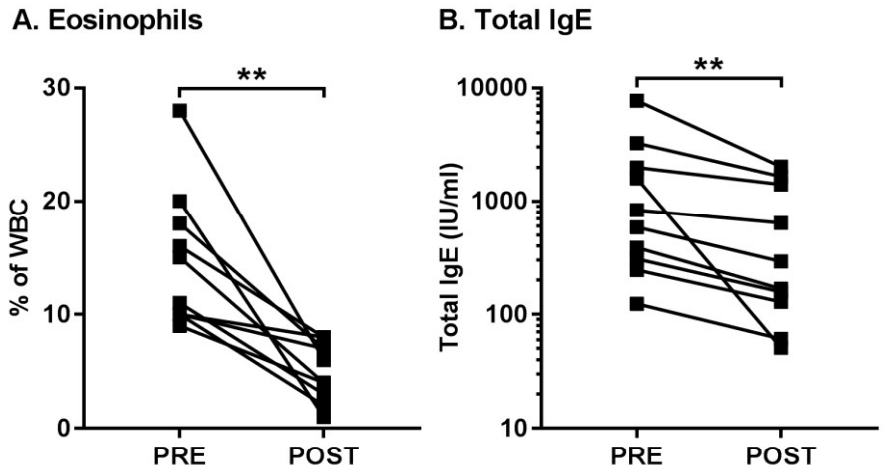

Fig. S2. Eosinophil counts and total IgE in rural Indonesians. (**A**) Eosinophil counts expressed as percentage of white blood cells (WBC) and (**B**) Serum measurements of total IgE of Indonesians pre- and post-anthelmintic treatment (n=10). ***P* <0.01 by paired student's t-test.

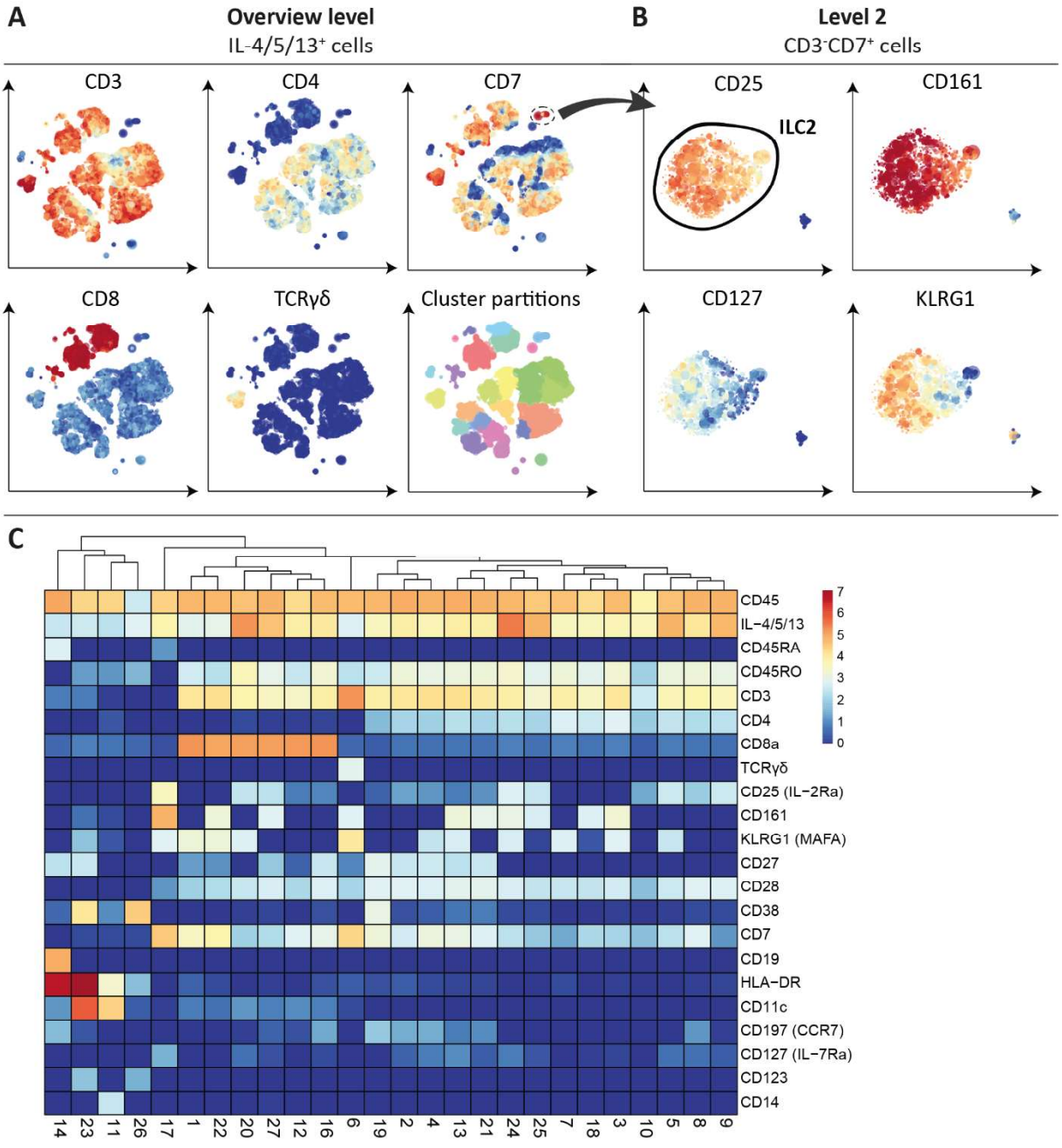

Fig. S3. Type 2 cytokine-producing cells. (**A**) First level embedding of IL-4/5/13^{+} cells from Europeans (n=10) and rural Indonesians infected with helminths (n=10), before and after 1 year of deworming, clustered on surface markers. Lower right panel shows cluster partitions of IL-4/5/13^{+} cells using GMS clustering. The expression of CD4 was reduced as a consequence of the stimulation. Color represents arsin5-transformed marker expression as indicated. Size of the landmarks represents AoI. (**B**) Second level embedding of the CD3^{-}CD7^{+} landmarks selected from the first level in fig. S3A, as indicated by the black circle, allowed the identification of ILC2s. (**C**) A heatmap summary of median expression values of cell markers expressed by IL-4/5/13^{+} cells identified in a. and hierarchical clustering thereof.

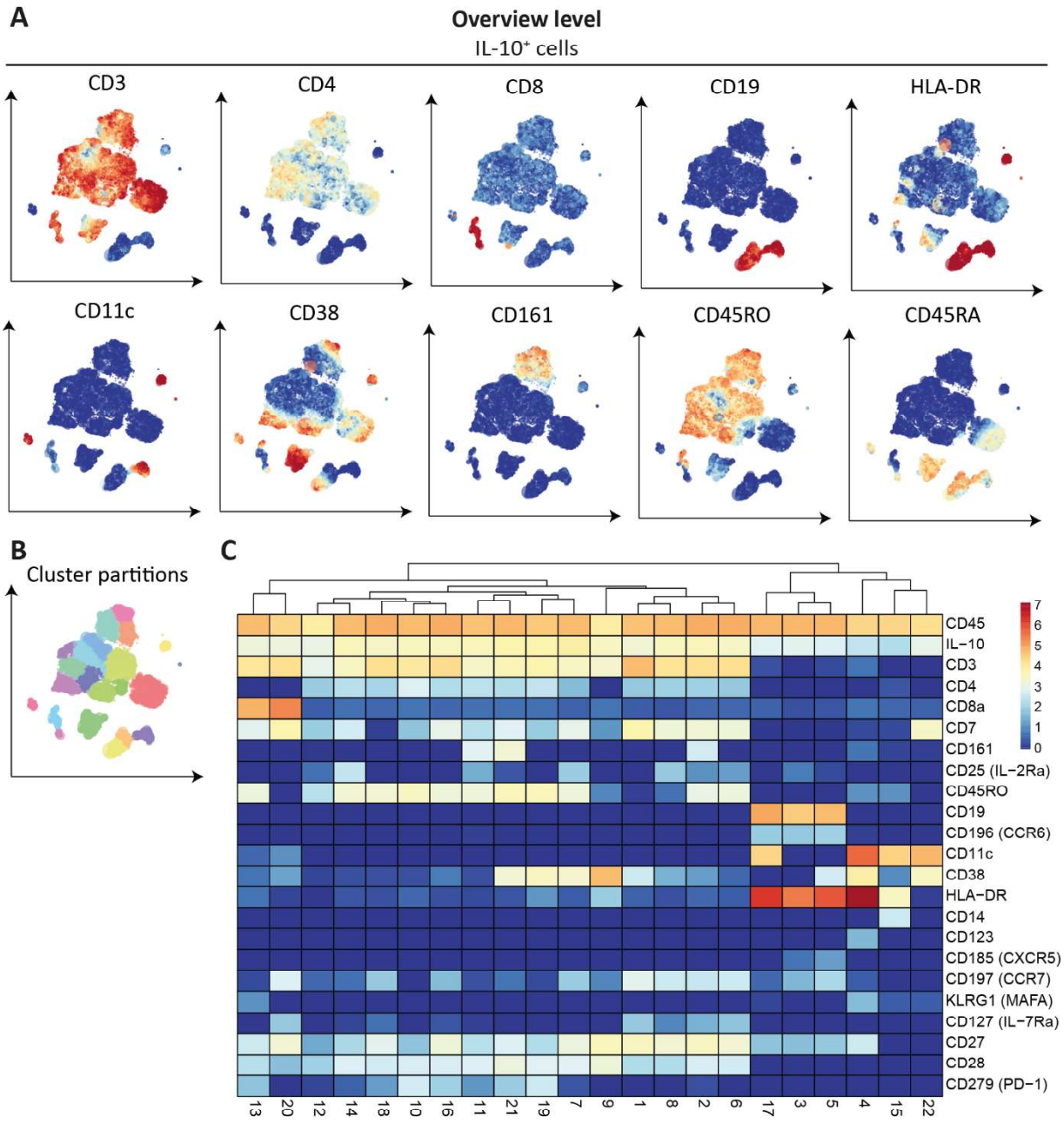

Fig. S4. IL-10–producing cells. (**A**) First level embedding of IL-10^{+} cells from Europeans (n=10) and rural Indonesians infected with helminths (n=10), before and after 1 year of deworming, clustered on surface markers. The expression of CD4 was reduced as a consequence of the stimulation. Color represents arsin5-transformed marker expression as indicated. Size of the landmarks represents AoI. (**B**) Cluster partitions of IL-10^{+} cells using GMS clustering. (**C**) A heatmap summary of median expression values of cell markers expressed by IL-10^{+} cells identified in fig. S4B and hierarchical clustering thereof.

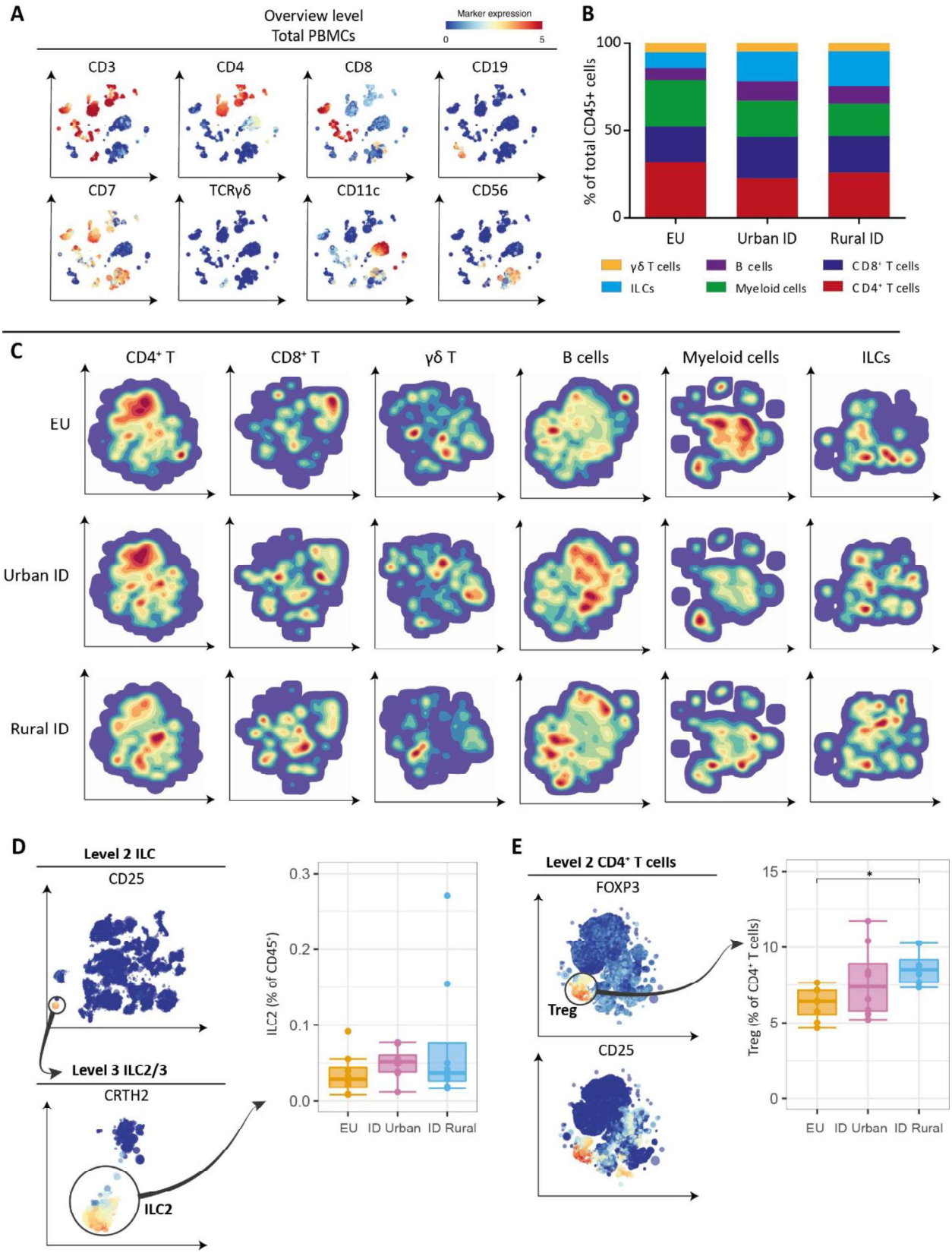
A
Overview level
Total PBMCs
Marker expression
0
5
CD3
CD4
CD8
CD19
CD7
TCRγδ
CD11c
CD56
B
100
50
0
% of total CD45+ cells
EU
Urban ID
Rural ID
γδ T cells
B cells
CD8⁺ T cells
ILCs
Myeloid cells
CD4⁺ T cells
C
CD4⁺ T
CD8⁺ T
γδ T
B cells
Myeloid cells
ILCs
EU
Urban ID
Rural ID
D
Level 2 ILC
CD25
Level 3 ILC2/3
CRTH2
ILC2
ILC2 (% of CD45⁺)
0.3
0.2
0.1
0.0
EU
ID Urban
ID Rural
E
Level 2 CD4⁺ T cells
FOXP3
Treg
CD25
Treg (% of CD4⁺ T cells)
15
10
5
0
*
EU
ID Urban
ID Rural

Fig. S5. Immune composition of Europeans and urban and rural Indonesians. (**A**) First HSNE level embedding of 14.3 million unstimulated cells. Color represents arsin5-transformed marker expression as indicated. Size of the landmarks represents AoI. (**B**) Comparison of lineage proportions relative to total cells between Europeans (EU, n=8)), Urban (n=8) and Rural (n=8) Indonesians (ID). (**C**) Density plots per lineage, stratified by sample origin, and therefore illustrating the differences and similarities between EU and Rural and Urban ID. (**D**) The top panel shows the second HSNE embedding of 2.2 million ILCs ($CD3^{-}CD7^{+}$), with color indicating CD25 expression. Cells within the black circle were selected and shown in the bottom panel is the third HSNE level embedding of the $CD25^{+}CD161^{+}CD127^{+}$ ILC. The right panel shows the frequency of ILC2s, indicated by black circle relative to total $CD45^{+}$ cells. (**E**) The left panels show the second HSNE level embedding of $CD4^{+}$ T cells, with color representing arsin5-transformed FOXP3 and CD25 marker expression as indicated. The right panel shows the frequency of Tregs relative to $CD4^{+}$ T cells. Differences between groups were tested with ANOVA followed by Tukey's post-test. *P <0.05.

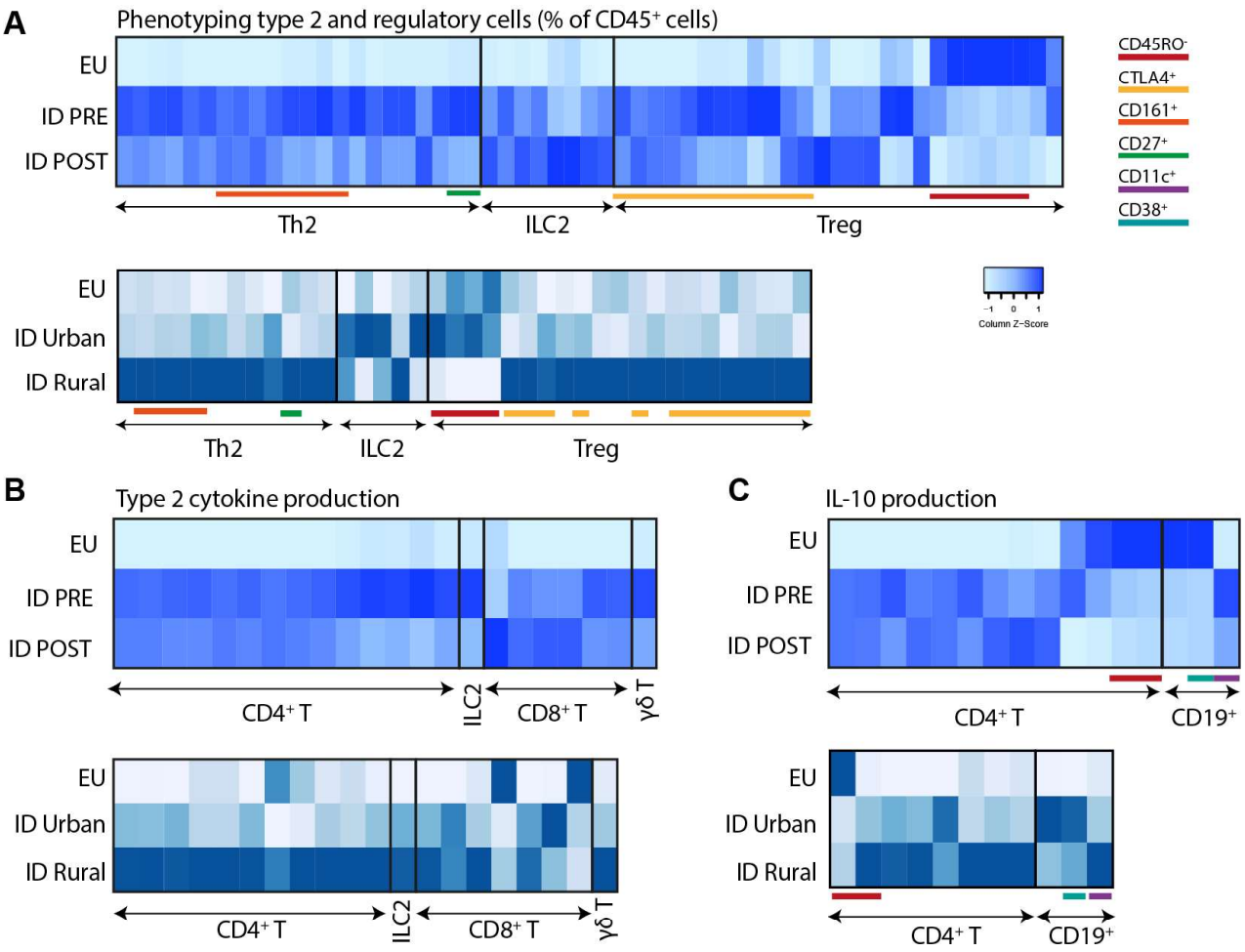

Fig. S6. Heat map summary. A heatmap summary showing the median cluster abundance of clusters identified in Fig. 2 (Th2), Fig. 3 (ILC2s), Fig. 4 (Tregs), Fig. 8 (second cohort including urban Indonesians), fig. S3 (type 2 cytokine-producing cells), fig. S4 (IL-10-producing cells) and fig. S5 (second cohort surface panel). Colored lines highlight a cluster(set) expressing a particular marker. Heatmaps are shown for both the first cohort (top) and the second cohort (bottom). (**A**) Cluster abundance relative to the number of $CD45^+$ cells. (**B**) Cluster abundance relative to the total number of its corresponding cell type (e.g. $CD4^+$ T cells, ILC2s, $CD8^+$ T or γδ T cells). (**C**) Cluster abundance relative to the total number of its corresponding cell type (e.g. $CD4^+$ T, $CD19^+$ B cells). EU, Europeans; ID Pre, Rural Indonesians pre-treatment; ID Post, Rural Indonesians post-treatment. ID Urban, Indonesians from urban centers; ID Rural, helminth-infected Indonesians from a rural setting.

Supplementary Tables

Table S1. Characteristics of the study cohorts.

Characteristic – first cohort	Europeans (n=10)	Indonesians (n=10)
Age, years (median, min, max)	32 (26-55)	36 (18-56)
Sex, female, *n*	5	5
Eosinophil count, %, (GM, min, max)	na	13.7 (9-28)
Total IgE, IU/mL, (GM, min, max)	na	823 (124-7753)
Helminth infection by PCR, No.		
Single	na	5
Multiple		5

GM, geometric mean; na, not applicable

Characteristic – second cohort	EU (n=8)	Urban ID (n=8)	Rural ID (n=8)
Age, years (median, min, max)	28 (22-32)	31 (18-37)	38 (18-54)
Sex, female, *n*	6	4	4
Eosinophil count, %, (GM, min, max)	na	na	13.5 (9-28)
Total IgE, IU/mL, (GM, min, max)	na	na	2498 (804-9999)
Helminth infection by PCR, No.	na	na	
Single			3
Multiple			5

GM, geometric mean; na, not applicable; EU, European; ID, Indonesian

Table S2. Helminth infection details of rural Indonesians.

Subject characteristics					PCR (Ct value)			
ID	**Cohort**	**Age**	**BMI**	**Sex**	**Al**	**Hw**	**Tt**	**Ss**
36	First	17	18.3	Male	Neg	28.4	33.4	Neg
449	First	55	21.1	Male	Neg	38.5	Neg	Neg
577	First	37	30.4	Female	Neg	Neg	32.3	Neg
596	First	55	19.6	Male	30.2	28.5	37.9	Neg
769	First	35	20.4	Female	25.6	27.8	28.5	Neg
897	First	46	26.8	Male	Neg	30.2	Neg	29.5
3702	First	18	17.6	Male	31.8	32.3	30.0	Neg
6324	First	35	19.5	Female	Neg	Neg	35.6	Neg
7200	First	28	20.2	Female	Neg	31.1	Neg	Neg
7878	First	24	21.8	Female	Neg	34.4	Neg	Neg
55	Second	18	16.3	Male	Neg	28.3	Neg	Neg
633	Second	38	20.9	Male	34.4	32.5	Neg	Neg
2147	Second	38	25.5	Female	Neg	Neg	34.3	Neg
2176	Second	54	20.8	Female	27.4	30.8	32.3	Neg
3460	Second	41	22.0	Female	Neg	41.3	Neg	Neg
3713	Second	53	26.1	Female	Neg	28.4	27.2	Neg
6106	Second	31	19.1	Male	Neg	30.3	34.1	31.7
7697	Second	31	18.7	Male	31.5	37.1	Neg	Neg

Samples were defined as negative by a Ct value of 50. The lower the Ct value, the higher the amount of DNA. Age of individuals is given in years. Abbreviations: Ct = Cycle threshold; Al = *Ascaris lumbricoides*; Hw = Hookworm; Tt = *Trichuris trichiura*; Ss = *Strongyloides stercoralis*.

Table S3. Antibody panel 1 (phenotyping).

Label	Specificity	Clone	Vendor	Catalogue number	Dilution
^{89}Y	CD45	HI30	Fluidigm	3089003B	200x
^{113}CD	CD45RA	HI100	eBioscience	83-0458-42	50x
^{141}Pr	CD196 (CCR6)	G034E3	Fluidigm	3141003A	100x
^{142}Nd	CD19	HIB19	Fluidigm	3142001B	200x
^{143}Nd	CD117 (c-Kit)	104D2	Fluidigm	3143001B	100x
^{145}Nd	CD4	RPA-T4	Fluidigm	3145001B	100x
^{146}Nd	CD8a	RPA-T8	Fluidigm	3146001B	200x
^{147}Sm	CD183 (CXCR3)	G025H7	BioLegend	353733	100x
^{148}Nd	CD14	M5E2	BioLegend	301843	100x
^{149}Sm	CD25 (IL-2Ra)	2A3	Fluidigm	3149010B	100x
^{150}Nd	CD185 (CXCR5)	J252D4	BioLegend	356902	100x
^{151}Eu	CD123	6H6	Fluidigm	3151001B	100x
^{152}Sm	TCRγδ	11F2	Fluidigm	3152008B	50x
^{153}Eu	CD7	CD7-6B7	Fluidigm	3153014B	100x
^{154}Sm	CD163	GHI/61	Fluidigm	3154007B	100x
^{155}Gd	CD278 (ICOS)	C398.4A	BioLegend	313502	50x
^{156}Gd	CD294 (CRTH2)	BM16	BioLegend	350102	50x
^{158}Gd	CD122 (IL-2Rb)	TU27	BioLegend	339015	100x
^{159}Tb	CD197 (CCR7)	G043H7	Fluidigm	3159003A	100x
^{160}Gd	FOXP3	PCH101	eBioscience	14-4776-82	50x
^{161}Dy	KLRG1 (MAFA)	REA261	Miltenyi	Special order	100x
^{162}Dy	CD11c	Bu15	Fluidigm	3162005B	200x
^{163}Dy	CD152 (CTLA-4)	BNI3	BioLegend	369602	100x
^{164}Dy	CD161	HP-3G10	Fluidigm	3164009B	100x
^{165}Ho	CD127 (IL-7Rα)	AO19D5	Fluidigm	3165008B	200x
^{166}Er	Tbet	4B10	BioLegend	644825	50x
^{167}Er	CD27	O323	Fluidigm	3167002B	200x
^{168}Er	HLA-DR	L243	BioLegend	307651	200x
^{169}Tm	GATA3	REA174	Miltenyi	130-108-061	50x
^{170}Er	CD3	UCHT1	Fluidigm	3170001B	100x
^{171}Yb	CD28	CD28.2	BioLegend	302937	200x
^{172}Yb	CD38	HIT2	Fluidigm	3172007B	200x
^{173}Yb	CD45RO	UCHL1	BioLegend	304239	100x
^{174}Yb	CD335 (NKp46)	92E	BioLegend	331902	100x
^{175}Lu	CD279 (PD-1)	EH 12.2H7	Fluidigm	3175008B	100x
^{176}Yb	CD56	NCAM16.2	Fluidigm	3176008B	100x
^{209}BI	CD16	3G8	Fluidigm	3209002B	400x

CCR, C-C chemokine receptor. CD, cluster of differentiation. CRTH2, prostaglandin D2 receptor 2. CXCR, CXC chemokine receptor. FOXP3, forkhead box P3. HLA-DR, human leukocyte antigen-D-related. IL-2R, interleukin-2 receptor. IL-7Rα, interleukin-7 receptor α. KLRG1, killer cell lectin-like receptor subfamily G member 1. MAFA, mast cell function-associated antigen. PD-1, programmed cell death protein. TCR, T-cell receptor. Markers in gray were stained intranuclear, while all other markers were stained on the cell surface.

Table S4. Antibody panel 2 (cytokine production).

Label	Specificity	Clone	Vendor	Catalogue number	Dilution
^{89}Y	CD45	HI30	Fluidigm	3089003B	200x
^{113}CD	CD45RA	HI100	Ebioscience	83-0458-42	50x
^{141}Pr	CD196 (CCR6)	G034E3	Fluidigm	3141003A	100x
^{142}Nd	CD19	HIB19	Fluidigm	3142001B	200x
^{143}Nd	CD117 (c-Kit)	104D2	Fluidigm	3143001B	100x
^{144}Nd	IL-2	MQ117H12	BioLegend	500339	400x
^{145}Nd	CD4	RPA-T4	Fluidigm	3145001B	100x
^{146}Nd	CD8a	RPA-T8	Fluidigm	3146001B	200x
^{147}Sm	CD183 (CXCR3)	G025H7	BioLegend	353733	100x
^{148}Nd	CD14	M5E2	BioLegend	301843	100x
^{149}Sm	CD25 (IL-2Ra)	2A3	Fluidigm	3149010B	100x
^{150}Nd	CD185 (CXCR5)	J252D4	BioLegend	356902	100x
^{151}Eu	CD123	6H6	Fluidigm	3151001B	100x
^{152}Sm	TCRγδ	11F2	Fluidigm	3152008B	50x
^{153}Eu	CD7	CD7-6B7	Fluidigm	3153014B	100x
^{154}Sm	CD163	GHI/61	Fluidigm	3154007B	100x
^{155}Gd	IFNγ	B27	BioLegend	506521	400x
^{156}Gd	CD294 (CRTH2)	BM16	BioLegend	350102	50x
^{158}Gd	CD122 (IL-2Rb)	TU27	BioLegend	339015	100x
^{159}Tb	CD197 (CCR7)	G043H7	Fluidigm	3159003A	100x
^{160}Gd	TNFα	MAb11	BioLegend	502941	400x
^{161}Dy	KLRG1 (MAFA)	REA261	Miltenyi	Special order	100x
^{162}Dy	CD11c	Bu15	Fluidigm	3162005B	200x
^{163}Dy	IL-17	BL168	BioLegend	512331	400x
^{164}Dy	CD161	HP-3G10	Fluidigm	3164009B	100x
^{165}Ho	CD127 (IL-7Ra)	AO19D5	Fluidigm	3165008B	200x
^{166}Er	IL-10	JES39D7	Fluidigm	3166008B	400x
^{167}Er	CD27	O323	Fluidigm	3167002B	200x
^{168}Er	HLA-DR	L243	BioLegend	307651	200x
^{169}Tm	IL-4	MP4-25D2	Fluidigm	3169016B	400x
^{169}Tm	IL-5	TRFK5	BioLegend	500829	400x
^{169}Tm	IL-13	JES105A2	BioLegend	504309	400x
^{170}Er	CD3	UCHT1	Fluidigm	3170001B	100x
^{171}Yb	CD28	CD28.2	BioLegend	302937	200x
^{172}Yb	CD38	HIT2	Fluidigm	3172007B	200x
^{173}Yb	CD45RO	UCHL1	BioLegend	304239	100x
^{175}Lu	CD279 (PD-1)	EH 12.2H7	Fluidigm	3175008B	100x
^{176}Yb	CD56	NCAM16.2	Fluidigm	3176008B	100x

CCR, C-C chemokine receptor. CD, cluster of differentiation. CRTH2, prostaglandin D2 receptor 2. CXCR, CXC chemokine receptor. HLA-DR, human leukocyte antigen-D-related. IL-2R, interleukin-2 receptor. IL-7Rα, interleukin-7 receptor α. KLRG1, killer cell lectin-like receptor subfamily G member 1. MAFA, mast cell function-associated antigen. PD-1, programmed cell death protein. TCR, T-cell receptor. Markers in gray were stained intracellular, while all other markers were stained on the cell surface.